Department of Physics and Astronomy
Heidelberg University

Bachelor Thesis in Physics
submitted by

Moritz Barth

born in Wiesbaden (Germany)

2023

Estimation of the Inelastic Muon Interaction Background for the SHADOWS Experiment

This Bachelor Thesis has been carried out by Moritz Barth at the
Kirchhoff Institute in Heidelberg
under the supervision of
Prof. Dr. Hans–Christian Schultz–Coulon

Abstract

The recently proposed SHADOWS experiment is designed to search for *feebly interacting particles* (FIPs) in the MeV to GeV range. It utilises the interaction of a 400 GeV proton beam delivered by the SPS at CERN with a beam dump, creating a variety of particles. These may include FIPs, a broad class of hypothetical particles with extremely suppressed couplings to Standard Model particles, which could explain phenomena such as Dark Matter. To reach an adequate statistical accuracy, the background has to be greatly reduced. This motivates a muon sweeping system and the off–axis positioning of the detector; the remaining inelastic muon interactions with the surrounding material are estimated in this work. For this purpose, data from Monte Carlo samples simulated by two different generators is analysed and compared. This involves several requirements for the interaction products so that they are indistinguishable from FIPs in the detector. The inelastic muon background over the 4 years of operation is found to be less than $2.45 \cdot 10^{-2}$ events for fully reconstructed vertices and $3.20 \cdot 10^{-1}$ events for partially reconstructed vertices. Moreover, a satisfactory level of agreement between the two samples is found.

Zusammenfassung

SHADOWS ist ein kürzlich vorgeschlagenes Beam–Dump–Experiment. Es ist für die Suche nach sogenannten *feebly interacting particles* (FIPs) im MeV bis GeV Bereich ausgelegt, wobei es den 400 GeV Protonenstrahl des SPS am CERN verwendet. FIPs sind eine weit gefasste Klasse hypothetischer Teilchen mit extrem unterdrückter Kopplung an das Standardmodell, welche Phänomene wie Dunkle Materie erklären könnten. Um eine hinreichende statistische Genauigkeit zu erreichen, ist eine starke Reduktion des Untergrundes notwendig. Dies erfolgt durch die Off–Axis–Positionierung des Detektors und ein Magnetsystem zur Ablenkung von Myonen. Die Abschätzung der verbliebenen inelastischen Wechselwirkungen von Myonen mit dem umliegenden Material ist Thema dieser Arbeit. Zu diesem Zweck werden die Daten von Monte Carlo–Simulationen mit zwei verschiedenen Generatoren ausgewertet und verglichen. Dies beinhaltet verschiedene Anforderungen an die entstehenden Produkte, sodass diese von FIP–Signalen im Detektor nicht zu unterscheiden sind. Der inelastische Myonenhintergrund über die Laufzeit von SHADOWS von vier Jahren wurde auf weniger als $2,45 \cdot 10^{-2}$ Ereignisse für vollständig rekonstruierte, und $3,20 \cdot 10^{-1}$ Ereignisse für teilweise rekonstruierte Vertices bestimmt. Des Weiteren wurde eine akzeptable Übereinstimmung zwischen den beiden Datensätzen gefunden.

Contents

1 | Introduction

Since ancient times, humankind has been searching for the 'truly uncuttable', culminating in Particle Physics, the study of fundamental particles and their interaction. The creation of particles requires high energies, naturally found in cosmic rays enabling physicists to identify the positron, muon and some light hadrons. Particle accelerators in the GeV range emerged in the 1950s, offering a new way to examine heavier particles rarely created in cosmic rays. With the introduction of the quark model in 1964, it became possible to classify the growing 'particle zoo' of hadrons. By the mid–1970s, the Standard Model (SM) was formulated as a theoretical framework describing the interactions between elementary particles. Although the SM successfully predicted several effects, a number of observations indicate its incompleteness.

Phenomena like Dark Matter, which cannot be explained with known particles, motivate the idea of extending the SM by incorporating new particles with small couplings to the SM particles. One newly proposed experiment dedicated to the search for these *feebly interacting particles* (FIPs) is SHADOWS, which would be located at CERN. A variety of particles is produced when the 400 GeV proton beam interacts with a beam dump, but the majority is absorbed instantly. Possibly produced FIPs in the MeV to GeV range[1] could be detected indirectly through their decay products. The background stems from muons, neutrinos and neutrons from the beam dump, in the form of inelastic interactions or random combinations of particles in the detector.

This work deals with the analysis of the inelastic muon scatterings with the detector material using data generated with a Monte Carlo simulation. The aim is to quantify the resulting particles and discuss different selection criteria that can be performed to lower the number of background events. The results are included in the Technical Proposal [1].

At first, a brief overview of the Standard Model, its limitations which motivate the concept of FIPs, and their detection mechanisms is provided in Chapter 2. The setup of the SHADOWS experiment and detector is outlined in Chapter 3. In Chapter 4, the implementation of the background Monte Carlo simulation is explained, while Chapter 5 discusses the created sample and the effect on the experiment in detail. Another sample was created with a different generator for validation, and both samples are compared in Chapter 6. The findings are summarised in Chapter 7.

[1]The mass range of MeV to GeV is derived from the possible production modes. SHADOWS expects FIPs below the B–meson ($\sim$5300 MeV) and above the kaon mass ($\sim$ 500 MeV).

2 | Theoretical Background

2.1 The Standard Model of Particle Physics

The Standard Model of Particle Physics (SM) is a theoretical framework describing all known elementary particles and three of the four fundamental forces acting between them [2]. It accurately describes the electromagnetic, strong and weak force, but does not include gravity. Since gravity is by far the weakest of the fundamental forces, its effect at atomic scales is negligible. On a theoretical level, the SM is a quantum field theory, which is invariant under local $SU(3)_C \times SU(2)_L \times U(1)_Y$ gauge transformation. For the scope of this work, a picture of elementary particles and forces between them mediated by gauge bosons will be sufficient.

The elementary particles are assumed to be point–like and are classified into *bosons* and *fermions*, according to their spin. For every particle exists an antiparticle with the same mass but opposite charge. A visualization of elementary particles in the SM and their respective interactions is depicted in Figure 2.1.

Bosons are characterised by integer spin. Whilst bosons with spin 0 are called scalar, spin 1 bosons are referred to as vector bosons. The latter act as force carriers, mediating momentum between particles, always conserving energy and momentum. The Higgs boson is the only scalar boson in the SM and plays a role in the mechanism of mass generation.

Apart from gravity which is not described by the SM, the only force actively encountered in everyday life is the electromagnetic force. It is mediated by the massless photon γ, and interacts with electrically charged particles. The gauge bosons of the weak interaction are the massive $W^{\pm}$ and Z boson, which couple to particles carrying weak charge, especially all fermions. The eight gluons g, also massless, are the mediators of the strong force, which couples to particles with colour charge. The respective quantities electric charge, colour charge, weak isospin and weak hypercharge are preserved under all interactions. The only exception is the interaction with the Higgs field, which does not conserve weak isospin and thus also not the weak hypercharge.

The Higgs boson H is an excitation of the Higgs field, which is crucial for the mass acquisition of all massive particles except for neutrinos. Fermions gain mass through the interaction of their respective fields with the Higgs field. However, the $W^{\pm}$ and Z bosons generate mass through electroweak symmetry breaking [4]. Not carrying electric or colour charge, the Higgs boson decays only via the weak force.

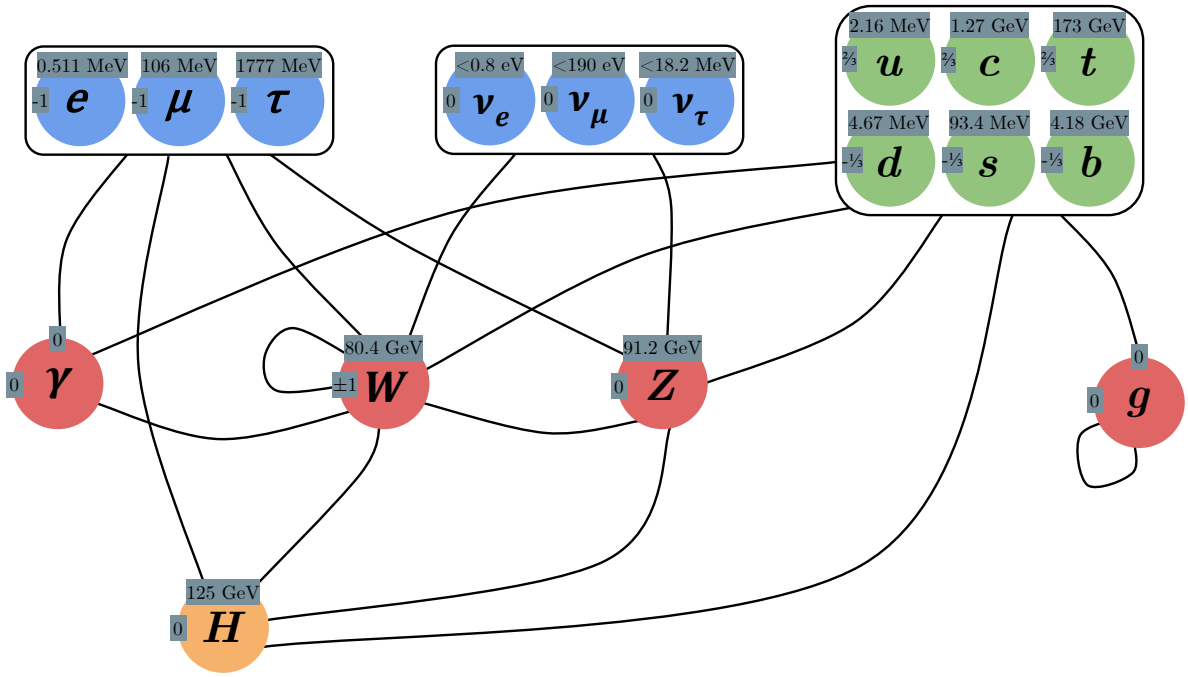

Figure 2.1: Elementary particles of the Standard Model. Lines connecting particles represent a possible interaction between them, their respective mass is depicted above the particle symbols and their electric charge on the left. Quarks (green) are charged under all SM forces. Leptons (blue) are divided into charged leptons (left) which interact via the electromagnetic and weak force, and neutrinos (right) which only interact weakly. Together, these two groups form the spin $\frac{1}{2}$ fermions. The spin 1 gauge bosons' (red) self-interaction is illustrated with a loop. The scalar Higgs boson (yellow) is crucial for the mechanism of mass generation, and is connected to all particles with mass apart from neutrinos. Specifications are taken from [3].

Fermions, with half–integer spin by definition, are subdivided into *quarks* and *leptons*. In addition to the up and down quark which make up all ordinary matter together with the electron, there exist two more variants of these two quarks, the only difference being their increased mass. The six quark flavours are divided into three *generations*, each consisting of an up–type quark (up u, charm c, top t) with electric charge $+\frac{2}{3}e$ and a down–type quark (down d, strange s, bottom b) with charge $-\frac{1}{3}e$. Quarks interact through all three forces, but flavour only changes in weak interactions via $W^{\pm}$ bosons. Due to colour confinement, quarks form *hadrons* under the strong interaction. One differentiates *mesons*, a bond between a quark and an antiquark, and *baryons*, consisting of three quarks or antiquarks[1]. While the mesons with the longest lifetime exist for a few nanoseconds, the proton, and the neutron in bound states, are stable baryons. The baryon number is a conserved quantity. An overview of the lifetimes of a few common particles is depicted in Figure 2.2.

[1]Recently, tetra– and pentaquark states have been observed at CERN [5, 6]. In general, a meson contains an even number of valence quarks, whereas a hadron with an uneven number of valence quarks is called a baryon.

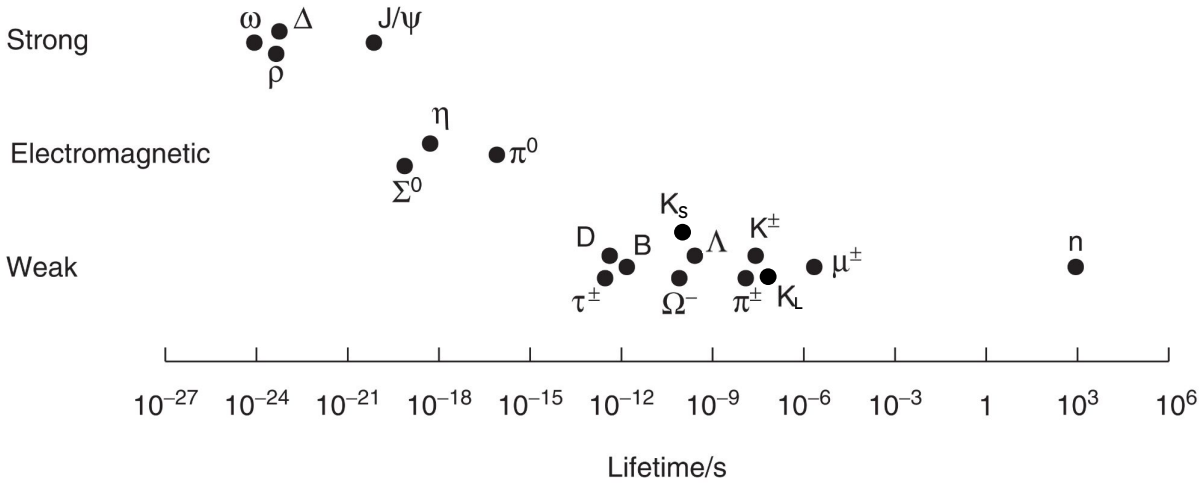

Figure 2.2: Lifetimes of common hadrons and leptons. The particles are arranged according to their predominant decay channel, which correlates with their lifetime. For reference, a highly relativistic particle with velocity near c requires about 40 ns to reach the SHADOWS decay vessel and 160 ns to pass the last muon station. Adapted from [2].

Leptons are similarly grouped into three generations, each containing a charged lepton (electron e, muon μ and tau τ) with an electric charge $-e$ and a corresponding, uncharged neutrino (ν_e, ν_μ, ν_τ). While the electron is stable, the heavier muon and tau decay into lighter leptons and mesons. Despite treated massless in the SM, the discovery of neutrino oscillations indicates that neutrinos do carry mass [7]. Neutrino oscillations also violate lepton family number conservation, so that only their sum, the lepton number, is conserved. Neutrinos exclusively interact weakly, and the SM does not incorporate right-handed neutrinos or left-handed antineutrinos, with the handedness being defined as the projection of the spin vector onto the momentum vector.

2.2 Beyond the Standard Model

Although the SM describes most observations precisely, several observation indicate it is incomplete, or has to be adjusted in some manner [8, 9]:

- *Neutrino oscillation*, as mentioned above, requires massive neutrinos, which is not implemented in the SM. Furthermore, it is not known how their mass is generated, as it is not done by the Higgs mechanism.

- *Baryogenesis* is a hypothesised process in the early universe, responsible for the matter–antimatter imbalance observed today. Assuming symmetric initial conditions and CPT conservation[2], neither of them should be dominant according to the SM.

- *Dark Matter* (DM), unlike ordinary matter, is characterised by being massive and not directly interacting with light. It is commonly assumed to have particle nature, but no SM particle fulfils all demands. Astrophysical observations of the cosmic microwave background, gravitational lensing and rotational curves of galaxies point to a source of mass that accounts for approximately 85% of the matter in the universe. The distribution of DM in the universe can be mapped precisely [11].

- The *strong CP problem* relates to the fact that charge conjugation and parity transformation seem to be preserved under the strong interaction, which is not necessarily enforced by the SM. Perhaps, processes violating the CP symmetry of the strong interaction simply have not been observed yet, or there lies some physical phenomenon underneath, which is not included in the SM.

Various theories address these issues by modifying the SM by introducing new particles into the framework, and thus tapping into the field of 'New Physics'. Over the last decades, many experiments have been dedicated to the search of a massive new particle in the range of several GeV to TeV, coupling to the weak force. The lack of results for such a WIMP (weakly interacting massive particle) has shifted the focus to lighter particles with small coupling to ordinary matter. Theories of those *feebly interacting particles* (FIPs) propose masses from sub–eV to GeV scales [8, 12].

A viable method of extending the SM with minimal modification is the introduction of a *dark sector*, containing multiple dark particles not charged under the SM forces, but interacting gravitationally with ordinary matter. In addition, DM and ordinary matter might interact via new couplings, called *portals*, and their respective mediator particles.

[2]The CPT theory states that a system behaves identical after charge conjugation (C), parity transformation (P) and time reversal (T), the three natural (near) symmetries of the SM. It is widely believed to hold true, although the single transformations are only approximate symmetries [10].

The theory heavily depends on the spin of the mediators, it the following is a brief overview of the most popular candidates:

- The *vector portal* requires a spin 1 mediator, with the most established one being the dark photon. It would interact with DM particles, and with SM matter only through kinetic mixing [13] with the ordinary photon[3]. Theory allows for heavy, light or even massless dark photons, however, it would be challenging to differentiate between the latter and the ordinary photon [14, 15].

- With similar mixing with the Higgs boson instead of the photon, a dark Higgs boson may interact with ordinary matter through the Higgs portal or *scalar portal*. Some theories propose multiple new Higgs bosons, or combine the dark Higgs boson with the dark photon portal [12, 16].

- Initially, the theory of axions was developed as a solution for the strong CP problem, but by now, axions or axion–like particles (ALPs) with greater masses, have evolved into popular dark matter candidates. They would correspond to the *pseudoscalar portal*, meaning they have spin 0 and odd parity, which is demanded by theory [9, 15], and can couple to photons, fermions or gluons.

- A possible explanation for the small neutrino masses is provided by the see–saw mechanism, which postulates a heavy fermionic partner to every neutrino type. Those are often referred to as heavy neutral leptons, right–handed or sterile neutrinos, as they would be uncharged under SM forces but mix with ordinary neutrinos. The integration into the SM would be realised via the *fermion portal* or neutrino portal [17].

Although the observation of one or even multiple of the aforementioned particles would be an enormous advance for Particle Physics, it would not resolve all the issues of the SM. These particles, in similar form, could arise as part of many much more wide–reaching theories, but the portal description gives a general structure for the new particle search within a limited parameter space.

[3] Others theories propose the dark photon coupling to the weak hypercharge of the electroweak theory, involving also mixing with the Z boson.

2.3 Detection of FIPs

The rising popularity of FIP theories has resulted in a wide landscape of experimental initiatives [8, 12] with energies ranging from sub–eV to several TeV. In the mass range of light dark matter from MeV to GeV, accelerators naturally pose the key method for experiments. The detection methods themselves can be categorised as follows [16]:

- The *detection of visible decay products* depends on the decay of FIPs into detectable SM particles such as photons, charged leptons or light meson pairs, which allows to infer the properties of the FIPs. Because of the long lifetime of FIPs, this method requires large decay volumes, but is feasible in beam dump and collider experiments.
- FIPs *scattering off the detector material* facilitates directly probing the properties of the FIPs. Both proton and electron beam dump experiments are viable, but it is difficult to distinguish the particles scattered off by FIPs and neutrinos.
- The *missing mass/momentum/energy method* aims to measure the properties of all visible products of an interaction, which allows to reconstruct the FIP properties through the missing component. A precondition for the missing mass method is knowing the momenta of the primary particles, and it is therefore mostly used in collider experiments. The missing momentum and energy methods also work in beam dump setups. All methods require precise measurements and a high sensitivity of the detectors.

A list of past, present and future experiments utilizing these methods can be found e.g. in [16]. SHADOWS relies on the detection of the decay products to reconstruct the properties of the FIPs.

3 | The SHADOWS Experiment

SHADOWS (**S**earch for **H**idden **A**nd **D**ark **O**bjects **W**ith the **S**PS) is a newly proposed beam dump experiment at CERN. It will explore the MeV to GeV mass range of FIPs, predominantly created in charmed and bottomed hadron decays. The experiment would be located in the North Area (see Figure 3.1), utilizing the 400 GeV proton beam from SPS with a centre–of–mass energy of $\sqrt{s} \approx 28\,\text{GeV}$ over four years of operation. Downstream of the beam dump, the experiment aims for the measurement of FIP decays using a large, off–axis decay volume and a full detector setup. In particular, the operation of the SHADOWS experiment is compatible with the proposed HIKE experiment [18], which will be located further downstream. HIKE will scrutinise rare decays of K^+ and K_0. This includes measuring branching ratios to high precision, the probing for decays forbidden by the SM, and the search for FIPs below the kaon mass, complementing the SHADOWS programme.

3.1 Beam Line and Experimental Site

The Super Proton Synchrotron (SPS) is the second largest particle accelerator in operation at the CERN complex, which is depicted in Figure 3.1. It is a synchrotron with a circumference of about 6.9 km, accelerating protons[1] up to energies of 450 GeV[2] after receiving them from the Proton Synchrotron (PS). Having started operation in 1976, a major success of the accelerator was the discovery of the W and Z boson in 1983 [20]. Today, the SPS serves as a pre–accelerator for the Large Hadron Collider (LHC) and additionally hosts a number of experiments itself.

The SHADOWS experiment [1, 22] would be located in the North Area, in the TCC8 target cavern before the ECN3 hall [19]. It will utilise the K12 beam line also used for the NA62 experiment [23], which begins after the beryllium T10 target for kaon experiments. A TAX (Target Attenuator for eXperimental areas) dump is located 23 m downstream of the T10 target, where it can act as a collimator for the K^+ beam for the NA62 or HIKE experiment and a beam dump for the remaining proton beam. It is possible to move the T10 target out of the beam and shift the TAX so that the entire beam is dumped. This is called the beam dump mode, opposed to the kaon mode.

[1] The SPS has handled a variety of particles over the decades, besides protons also antiprotons, ions, electrons and positrons.

[2] Fixed target operations like SHADOWS only utilise a 400 GeV beam, to ensure a longer beam extraction time ('flat top') [19].

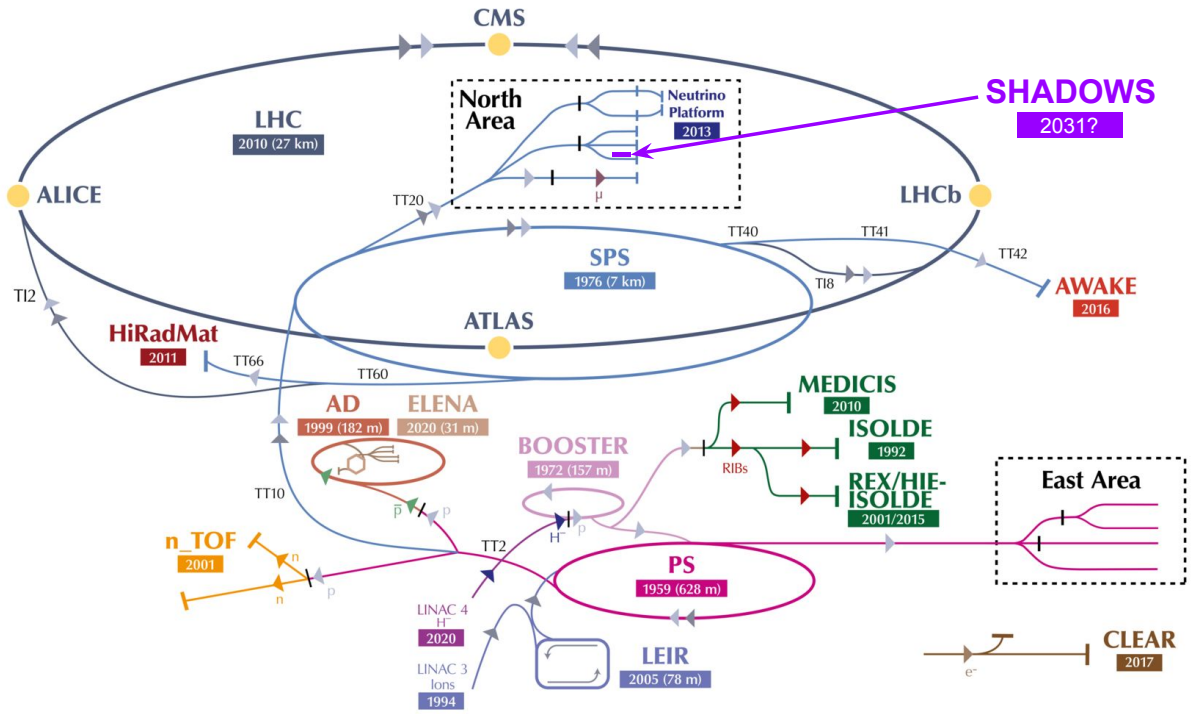

Figure 3.1: The CERN accelerator complex as in 2022. The SHADOWS experiment is located in the North Area, which is fed by the SPS. The protons injected into the SPS have been pre–accelerated in the Linac4, the PSB and the PS. Adapted from [21].

SHADOWS will be operated in beam dump mode, expecting a proton intensity of $2.0 \cdot 10^{13}$ protons on target (pot) per spill. A spill refers to all protons from the SPS which are directed on the TAX dump, before the synchrotron ring is refilled. For the $2.4 \cdot 10^{6}$ spills expected in the SHADOWS lifetime, that makes about $5 \cdot 10^{19}$ pot events over the duration of the experiment.

3.2 Beam Dump and Muon Sweeping System

The copper–iron TAX with a thickness of about $\lambda_{\text{int}} = 22$ nuclear interaction lengths is sufficiently long to absorb most of the hadrons and electromagnetic radiation, leaving neutrons, muons, neutrinos and potentially FIPs. For radiation protection, it is encased in iron and concrete shields (see Figure 3.2).

The background primarily originates from muons, either through inelastic interaction with the detector material or through combinatorial background (see Section 4.1). Therefore, a muon sweeping system consisting of multiple Magnetised Iron Blocks (MIBs) is installed. On the one hand, the muons lose energy simply by moving through the blocks (passive mitigation), so that especially low-momentum muons do not reach the detector acceptance region. On the other hand, the charged muons are swept away from the detector (active mitigation). The Stage 1 magnet separates the muons and antimuons, which are then

pushed out of the detector acceptance region by the Stage 2 and Stage 3 magnets, as shown schematically in Figure 3.3.

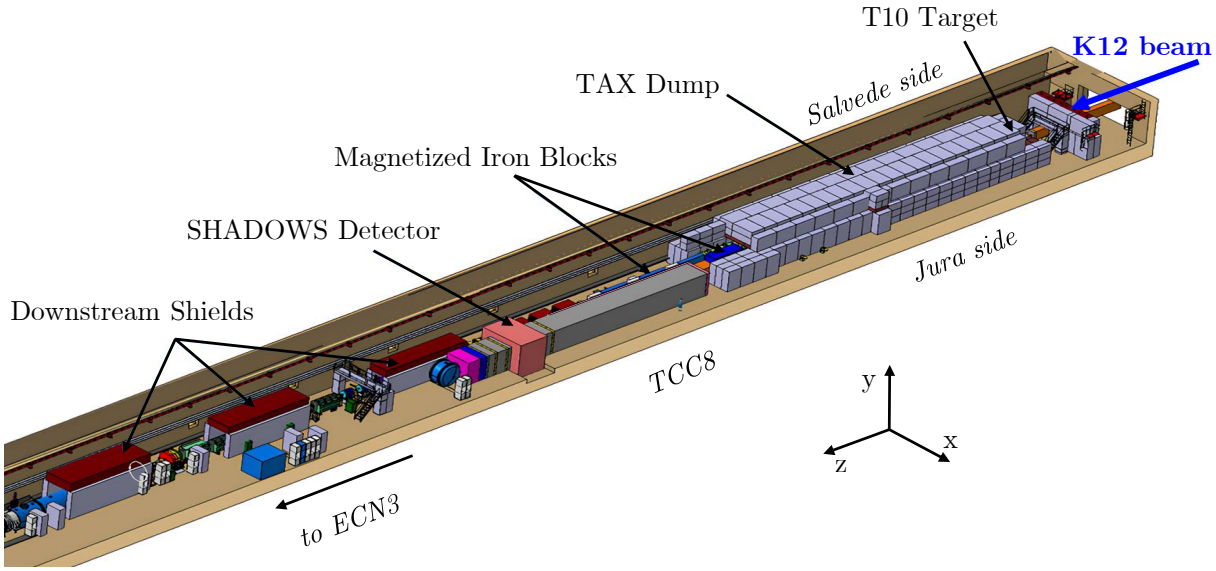

Figure 3.2: Sketch of the TCC8 tunnel. The beam line, the shielding around the beam dump, the MIBs and the SHADOWS detector are visible. Adapted from [24].

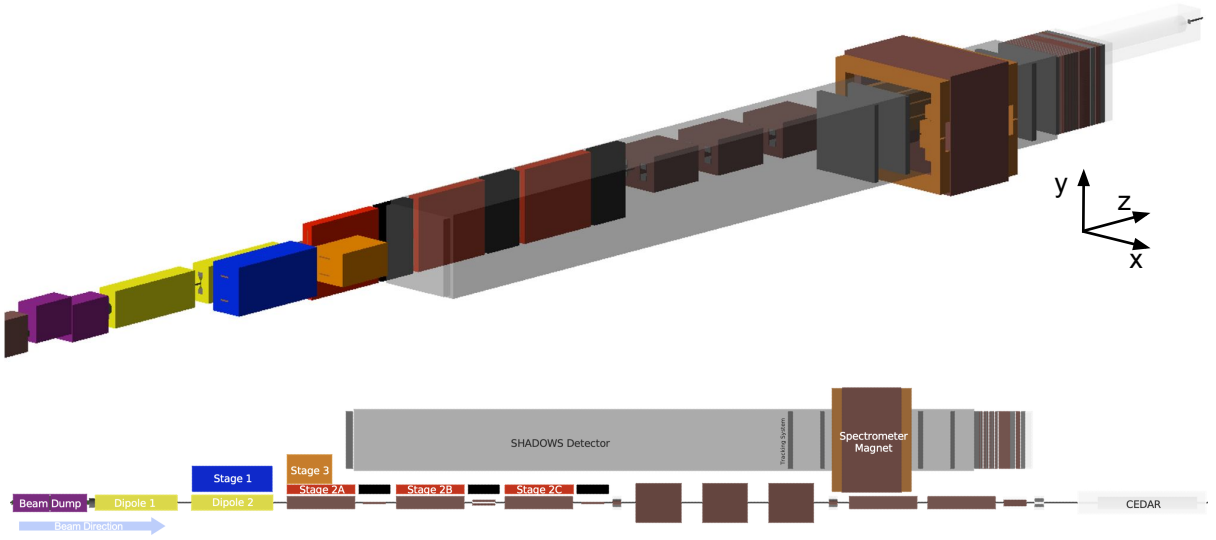

Figure 3.3: The MIB system at the beam line. Stage 1 (blue) separates the muons by charge. Stage 2 consists of three MIBs (red) alternating with iron shields (black) to sweep the muons away from the decay volume in y–direction. Stage 3 (orange) pushes the muons further and serves as a detector cover. Taken from [1].

3.3 The SHADOWS Detector

The objective of the SHADOWS detector is to identify most of the products from FIP decays whilst reducing the background to a minimum.

At the given energies, FIPs are expected to leave the beam dump under a wide opening angle, whilst only low–momentum muons and neutrinos do so as well. This motivates the off–axis positioning of the detector, which is planned to be about 1.5 m in x–direction. A schematic view of the detector is depicted in Figure 3.4. In the following, the different sub–detector systems are briefly explained [1].

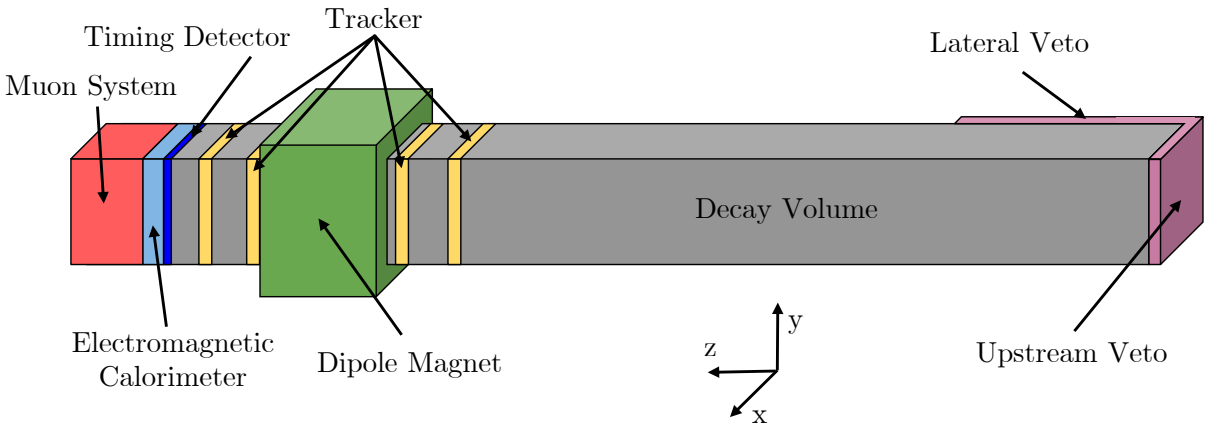

Figure 3.4: The SHADOWS detector. The decay volume is covered by the veto system next to the beam. The tracking system with the dipole magnet, the timing detector, ECAL and muon system allow to reconstruct FIP decays whilst reducing the background.

Decay vessel The cuboidal decay vessel would be made of 14 mm thick ferro–pearlitic structural steel holding a vacuum of 1 mbar [25]. In the SHADOWS coordinate system depicted in Figure 3.5, it starts at $z = 38.05$ m and ranges up to $z = 67.25$ m, having an aperture of 2.5 m $\times$ 2.5 m. It contains the four tracking stations and is interrupted by a dipole magnet from $z = 60.9$ m to $z = 64.5$ m.

Veto system To reduce the muon background, the aperture and a large part of the vessel wall alongside the beam are planned to be covered by a veto system. This would be realised with MicroMegas detector modules, which provide sufficient spatial and time resolution under the given radiation level and have a detection efficiency of about 98%. A double layer layout has been proposed, and studies yield a 99.8% efficiency for muons [26].

Tracking system The SHADOWS tracking system consists of two tracking stations before and two after a dipole magnet to precisely determine the tracks and momenta of charged particles. This allows to reconstruct the potential FIP decay vertices and masses. The dipole magnet will have the approximate dimensions of 2.7 m $\times$ 2.7 m $\times$ 3.3 m and

provides an integrated field of 0.9 Tm between the tracking stations, which bends the particle tracks in x–direction according to their mass and charge. Each of the tracking stations consists of two stereo layers of straw drift tubes, one in x–direction and one in y–direction, with a combined tracking efficiency of more than 98%.

Timing detector To reduce the combinatorial muon background (see Section 4.1), a timing detector reconstructs whether particles are produced in the same vertex. It is intended to use two arrays of about 50 scintillating bars each for the x and y–direction. Each bar is read out by 8 SiPMs (Silicon PhotoMultipliers) on both ends, giving a total of 1600 SiPMs. The entire detector will have a timing resolution of approximately 80 ps.

Electromagnetic calorimeter To reconstruct especially the FIP decay into two photons, an electromagnetic calorimeter (ECAL) with pointing capability is required. The favoured design is a sampling calorimeter with alternating iron or lead absorbers and scintillating strips as active layers. A depth of $X_0 = 20$ radiation lengths guarantees containment of the full showers from high energy photons. This requires 40 layers of iron and 40 active layers with 250 scintillating strips each.

Muon system The muon system assists the timing detector to distinguish between the combinatorial muon background and the expected muons from FIP decays, and therefore requires a good timing resolution. This is met by plastic scintillator tiles read out by SiPMs. Either 16 or 32 tiles are combined into one module, and 8 or 16 modules make up one muon station. Three muon stations are planned, separated by iron filters.

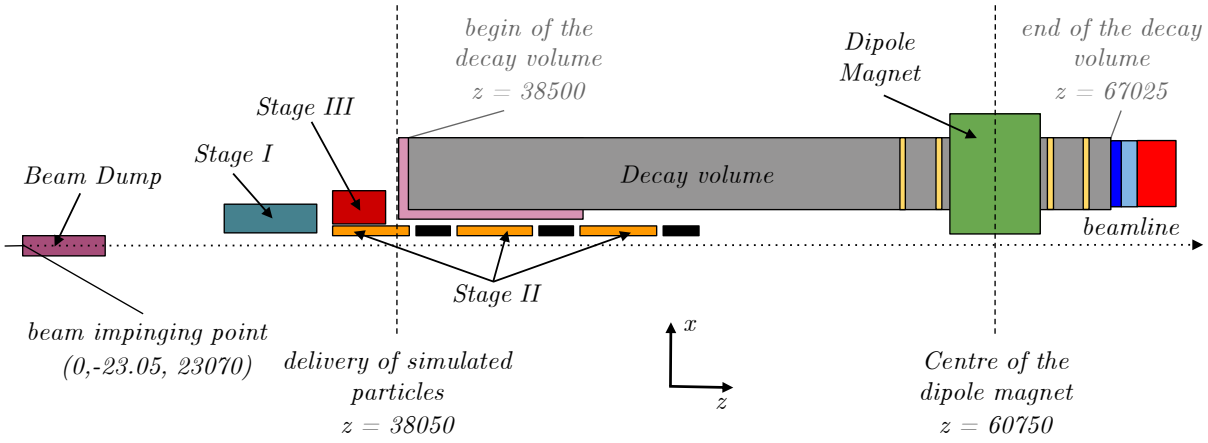

Figure 3.5: The SHADOWS coordinate system and detector dimensions projected on the xz–plane. All specifications are given in mm. The whole detector is set off–axis by 2612 mm in x–direction, and is symmetrical in the y–direction around $y = 0$. As origin, the impinging point of the proton beam with the T10 target is chosen, the TAX dump is located 23 m downstream. The decay volume ranges from $x = 1370$ to $x = 3920$, $y = -1280$ to $y = 1280$, and $z = 38\,500$ to $z = 67\,025$.

Trigger and data acquisition system Data digitisation and transmission, data buffering, selection and storing are combined in the Trigger and Data Acquisition System (TDAQ). Triggering is required to reduce the enormous amount of data to the events which are relevant for the FIP search. Depending on the radiation level, different radiation–hard ASICs (Application Specific Integrated Circuits) or FPGAs (Field Programmable Gate Arrays) are considered for the detector readout and data digitisation. The unfiltered data is transported about 100 m away from the detector using a lpGBT (Low Power GigaBit Transceiver) link, which also provides a clock signal to the detectors. The signal is read out by the off–detector electronics such as FELIX (Front End LInk eXchange) cards and sent to a subsequent buffer. It is planned to avoid on–detector triggering, which means that the buffer must hold the data of an entire spill. However, this allows to adjust or change the trigger and data taking at a later stage. After selecting and triggering the events of interest and event building, the data is stored permanently.

4 | Background Simulation

A Monte Carlo (MC) simulation of the full SHADOWS setup is implemented in the NA62 Monte Carlo framework based on the GEANT4 simulation software [27, 28], which is capable of simulating particle interactions with the detector. It has been used to generate a signal sample to investigate the FIP acceptance rate, as comparison with measured muon flux data, and for samples examining the muon and neutrino background. This work analyses the inelastic muon interactions; the sample creation and techniques for this case are described below.

4.1 Background Effects

The background of the SHADOWS experiment is dominated by muons, neutrons and neutrinos, as they are mostly not absorbed in the beam dump. They might account for fake signals, which are misidentified as FIPs and distort the results. The off–axis positioning of the detector reduces all background effects, because most particles and especially those with high momentum are produced at small angles relative to the incoming beam.

Neutrons with up to 100 MeV originating from interactions in the beam dump only pose a relevant background to the ECAL. There, they can be identified by a small penetration depth compared to other particles, which is due to their low momentum. The other component of the neutron background are thermal neutrons with energies in the range of a few eV. The detectors are not sensitive to the uncharged low–energy neutrons, but as they interfere with the electronics, it might be mandatory to install shieldings.

The neutrino background results from deep inelastic scatterings (DIS) with the surrounding material, in particular with the decay vessel. These scatterings produce mainly leptons and light mesons, which can account for FIP-like secondary decays. However, the neutrino component of the background is expected to be small due to their small interaction cross–section and the low momenta of the secondary interaction products.

Muons contribute to the background in two ways:

- *Combinatorial* background originates from unrelated, oppositely charged muons hitting the detectors at about the same time and mimic a signal event. Most of the random combinations are eliminated by the timing detector and muon system. The misidentified events can be further reduced by the veto system and different selection criteria, e.g. demanding the reconstructed vertex to be in the decay volume and the fake FIP signal to originate close to the beam dump.

- *Deep inelastic interactions* of muons with the protons in the set–up can create particles mimicking FIP signals, similar to neutrinos. However, the larger cross–section drastically increases the number of expected interactions. The veto system identifies muons before they interact with the decay vessel and the same selection criteria as to the combinatorial background can be applied. Still, the inelastic muon interactions account for the largest background component, and their analysis and quantification are the subject of this thesis.

4.2 Sample Creation

Due to varying demands on the simulation, different software packages are used to deal with different segments of the set–up. The interaction of the proton beam with the TAX dump and the subsequent MIB system is simulated with the GEANT4–based `BDSIM` (`Beam Delivery Simulation`) software [29]. The particles surviving the sweeping system with energies over 3 GeV[1] are handed over to the full SHADOWS MC simulation at $z = 38.05\,\mathrm{m}$, which operates with GEANT4. Here, the whole setup with the vessel and the detectors is implemented as described in Section 3.3. A schematic of the coordinate system of the MC simulation with the used detector geometry is shown in Figure 3.5.

To increase the number of events in the sample whilst reducing computing time, the *muon biasing technique* [30] was applied. It starts with a proton from the beam which interacts with the TAX dump producing some secondary particles like mesons and photons. These particles are cloned, with the clones having the same momenta as the original particles. If the original particles create more particles before they decays or leave the beam dump, they are cloned as well. Then, the cloned particles are simulated, but the cross section of all processes which would not produce muons is set to zero. The interaction length of the particles is decreased artificially until a muon is created, and the cloned particle replaces the original one. To compensate for that, a probability weight (see Section 5.3) is added to the muons. The sample created from the simulation restricted to muons was used for the inelastic muon interaction study, and will be referred to as GEANT4 sample. It is equivalent to $9.28 \cdot 10^{11}$ pot events.

Another sample was created with the PYTHIA6 generator [31], which describes interactions involving charm and strange quarks better than GEANT4, whose main purpose is to simulate the passage of particles through matter. In order to further increase the statistical power of the sample, the muons surviving the sweeping system have been forced to exclusively interact with the decay vessel in DIS, which is expressed by another weight. The resulting sample will be referred to as PYTHIA6 sample and is equivalent to $1.51 \cdot 10^{19}$ pot events.

[1] The value of 3 GeV originates from the same threshold value of the trackers, meaning that particles with momenta below 3 GeV are not tracked anyway and thus cannot be mistaken for FIP signals.

5 | Analysis of the Pythia6 Sample

The sample created with PYTHIA6 forced muons to interact with the decay vessel if possible, with the goal of quantifying the inelastic muon interaction background. Interactions with the vessel pose a majority of the background, because particles are created behind the veto system directing into the decay volume. The data set contains the muon scattering events from $1.285 \cdot 10^8$ simulated proton on target (pot) events.

5.1 Sample Composition

For easier handling, the sample was converted from the GEANT4–output into analysis trees in the form of `ROOT` TTrees [32]. These trees have an entry for every scattering event, and each of them contains the variables listed in Table 5.1.

Table 5.1: Variables in each event of the Pythia6 trees. The data type of continuous values is `double` with a precision of approximately 16 decimal digits, which is well under the GEANT4 step–size.

Variable name	Description
multiplicity	number of particles participating in the interaction, i.e. initial, intermediate and final particles
event ID	unique number given to the pot events in one single file
event weight	weight from the muon biasing technique
muon weight	weight from the forced interaction with the decay vessel
p_x, p_y, p_z	momentum components of the particles
x, y, z	position of the interaction
particle code	particle type according to the MC numbering scheme [33]

The events are separated into 257 files, with each file containing the created particles from 500 000 pot events. Of the $1.285 \cdot 10^8$ simulated pot events, $3.60 \cdot 10^7$ muons hitting the vessel were produced with the muon biasing technique. Only $7.12 \cdot 10^5$ of these interactions are deep inelastic scatterings (DIS), i.e. the proton structure breaks up and new particles are created. These muons are identified by a multiplicity greater than 1 and muon weight smaller than 1 and are the basis of the following analysis.

A typical muon inelastic scattering event is shown in Table 5.2. The internal operating mode of PYTHIA6 is visible: The entries are ordered by time, so that the first entry is the incoming muon, followed by the proton it interacts with, each with their initial momenta. After this the exchange process starts, in which a photon mediates momentum between the two particles and the proton structure breaks up. A string or cluster is created, which arises from hadronization theories. It confines all quarks and then decays to hadrons,

which can decay further. Alternatively, a heavy hadron (e.g. ρ^0, ω or ϕ) is created instead of the string or cluster, and decays subsequently. Both processes raise the problem of the instantly decaying particles and states appearing in the event and thus in all statistics. This makes a method to distinguish between temporary and final particles crucial.

5.2 The Final Particle Algorithm

In the context of this thesis, an algorithm to identify the final particles of the interactions was developed and used for the Technical Proposal. It assigns a flag to every particle, whether it is temporal or final. The realization is discussed in the following in detail, an example event is illustrated in Table 5.2.

Initially, all particles are marked as 'final' except for the initial muon and proton. The algorithm then iterates over all particles, and probes all subsequent particles[1], consecutive pairs, triplets or quadruplets (only for the $\eta \to \pi^+\pi^-e^+e^-$ decay). If they match the energy and momentum of the original particle, its flag is set to temporal. Some fine–tuning is required to decide how precisely the momenta and energies must fit. Starting at perfect agreement, the momentum and energy requirements were lowered, until all decays were identified. This resulted in demanding all three momentum components to fit by 1%, and for the particle transformations additionally a 10% energy agreement.

In the last step, the energies of all final particles are summed up and subtracted from the energy of the incoming muon and proton, which should yield a value close to zero. If the energy sum is above 2 MeV, all particle energies are compared to the remaining energy and momenta, and their flag is flipped if the energies and momenta match[2].

A challenge is posed by mediator particles, quarks, diquarks, clusters and strings, whose masses are unknown or whose momenta tend not to fulfil momentum conservation. As they are not expected to be final particles, these particles are initially flagged as temporal. Photons however can also be final particles and are consequently flagged as final whenever they are created in a decay.

Results from the algorithm have been examined carefully. The agreement of momenta and energies for incoming and outgoing particles is tested using the momentum and energy sums, which are expected to be close to zero. The sum of the p_x and p_y momenta is typically less than 10^{-12} MeV, for p_z momenta below 10^{-2} MeV, and the energy sum rarely surpasses 1 MeV. In addition, many events have been reconstructed by hand and were compared with the output of the algorithm.

[1] The reason for iterating over all single particles is to identify transformations like K^0 to K_L or particle reappearances e.g. initial particles before and after initial state radiation.

[2] This is necessary due to of the effect of some QCD effective states, which causes single particles to have no conserved momenta and energies. Apart from that, it corrects for randomly fitting momenta.

Table 5.2: A typical event evaluated with the final particle algorithm. Total momentum and particle energy are calculated for convenience. The column labelled 'final' indicates whether a particle remains after interaction or is only an intermediate particle.

event ID	3621					
multiplicity	25					
event weight	0.000130449					
muon weight	4.27217e-09					
position [mm]	$x = 1356.08$	$y = -43.1573$	$z = 59\,413.5$			
part.	p_x [MeV]	p_y [MeV]	p_z [MeV]	p [MeV]	E [MeV]	final
μ^+	230.142	-31.2744	4412.35	4418.46	4419.73	0
p^+	0	0	–4.44089e-13	4.44089e-13	938.272	0
μ^+	–275.57	201.092	2625.05	2647.12	2649.23	0
γ	275.518	–201.054	1793.08	1825.23	1825.23	0
p^+	0.0522942	–0.0381607	0.340332	0.346434	938.272	0
γ	345.505	–252.125	2248.55	2288.87	2288.87	0
u	–3.27564	2.39033	–21.3179	21.7002	21.8217	0
γ	345.505	–252.125	2248.55	2288.87	2288.87	0
u	–3.27564	2.39033	–21.3179	21.7002	21.8217	0
u	342.229	–249.735	2227.24	2267.17	2267.17	0
μ^+	**–275.57**	**201.092**	**2625.05**	**2647.12**	**2649.23**	**1**
u	–18.7001	488.564	1685.64	1755.11	1755.11	0
ud_0	294.27	–689.656	107.779	757.52	953.656	0
string	275.57	-201.092	1793.42	1825.57	1825.57	0
ω	9.48659	67.1632	1435.62	1437.22	1636.51	0
p^+	**266.084**	**–268.255**	**357.795**	**520.364**	**1072.91**	**1**
π^-	52.9441	–103.546	86.3845	144.869	201.164	0
π^+	128.582	17.9815	822.23	832.418	844.037	0
π^0	–172.04	152.727	527.008	575.031	590.66	0
μ^-	**65.1624**	**–70.9479**	**84.9672**	**128.449**	**166.321**	**1**
$\overline{\nu_\mu}$	**–12.2183**	**–32.5976**	**1.41727**	**34.8411**	**34.8411**	**1**
μ^+	**83.3248**	**29.6503**	**694.206**	**699.817**	**707.748**	**1**
ν_μ	**45.2576**	**–11.6688**	**128.024**	**136.289**	**136.289**	**1**
γ	**–125.048**	**42.5605**	**177.892**	**221.572**	**221.572**	**1**
γ	**–46.9917**	**110.167**	**349.116**	**369.089**	**369.089**	**1**
sum	–9.237e-14	1.137e-13	–2.175e-4		–2.080e-3	

To conclude, the algorithm always identifies the final particles of the inelastic muon proton interactions correctly.

5.3 Nature of the Interactions

The final particles of the $7.12 \cdot 10^5$ deep inelastic muon interactions can be identified using the algorithm described in the previous section. To understand how these events can be misidentified as FIP signals, it is crucial to examine them further.

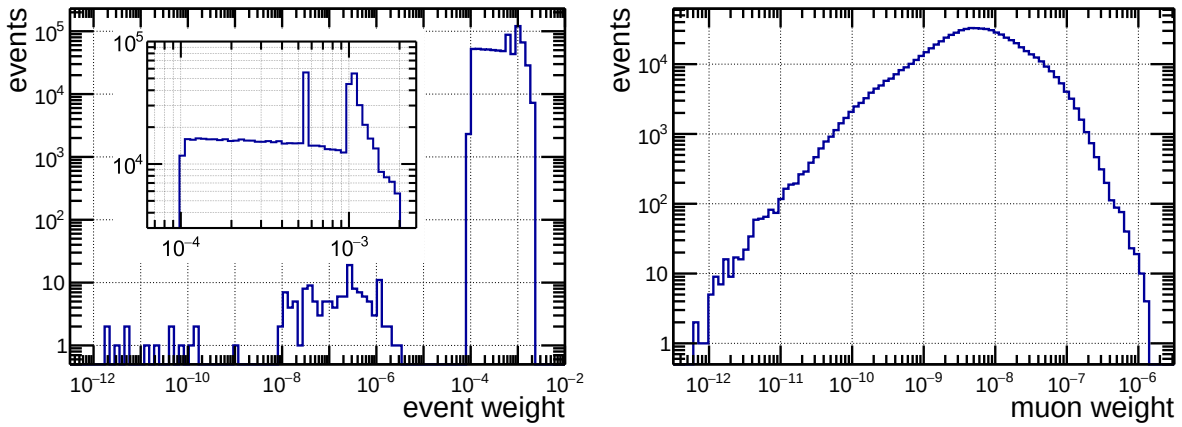

Figure 5.1: Event and muon weight of the Pythia6 sample. The event weight (left) is on average $6.29 \cdot 10^{-4}$, the muon weight (right) has a mean of $1.35 \cdot 10^{-8}$.

Event Weight and Muon Weight

Each event of this sample is assigned two weights, the *event weight* resulting from the muon biasing and the *muon weight* arising from the forced interaction with the vessel. Both weight distributions are depicted in Figure 5.1. For the vast majority of events, the event weight is between 10^{-4} and 10^{-2} with an average of $6.29 \cdot 10^{-4}$. Smaller weights stem from events with multiple initial particles not included in the sample, and each of them contributes with a factor from the biased proton interaction. This will be described in more detail in Section 6.3.

The muon weights range continuously from -12 to about 10^{-6} with an average of $1.35 \cdot 10^{-8}$ and the peak slightly after. The standard deviation of the distribution is $\sigma = 2.82 \cdot 10^{-8}$. Neither the event nor the muon weight shows a position dependence, and the distribution of the event weights does not differ significantly from the sample before filtering out muons which did not interact deep inelastically. There is also no correlation between the two weights.

With the average weight, the number of pot events the sample is equivalent to can be calculated by dividing the sample size by the weights. This results in $1.51 \cdot 10^{19}$ pot events, which is slightly about a third of the expected pot events over the SHADOWS lifetime.

Multiplicity and Particle Content

After the final particle algorithm has identified the resulting particles of the interactions, there is a clear structure in the multiplicity, depicted in Figure 5.2. Even multiplicities occur more often than odd ones by about a factor of 10. The reason for this lies in the particle composition, which can be seen in Table 5.3.

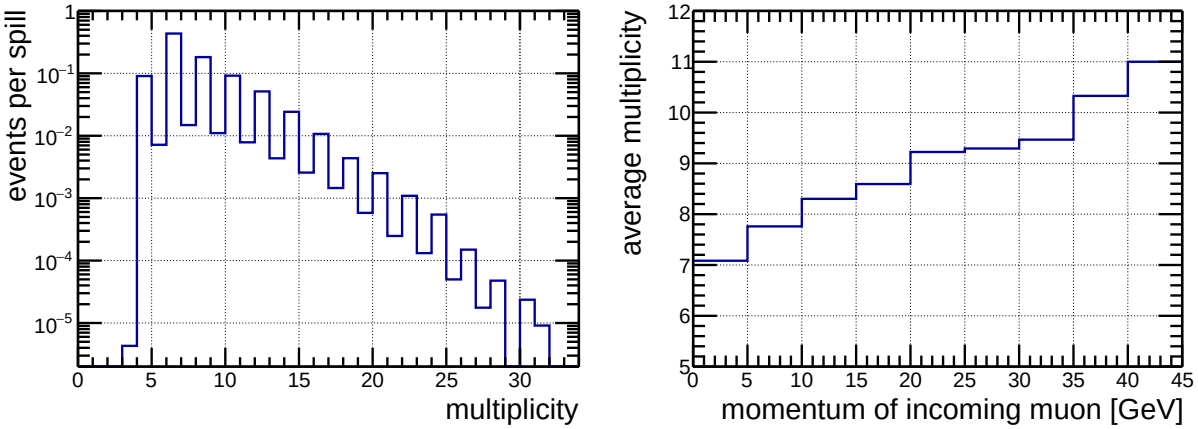

Figure 5.2: Multiplicity of the Pythia6 sample. The number of final particles (left), including the scattered muon and proton, ranges from 3 particles (Compton scattering) to fairly complex showers with up to 31 final particles. Multiplicity and momentum of the incoming muon are correlated (right), with higher initial momenta creating more interaction products. The average multiplicity is 7.5.

Table 5.3: Particle content of the Pythia6 sample. The initial muon and proton are also included.

particle	counts	part./spill	particle	counts	part./spill
p	540 204	0.68	$\overline{p}$	255	0.0012
n	172 192	0.27	$\overline{n}$	247	0.0012
μ^-	915 811	1.20	μ^+	1 050 351	1.56
ν_μ	712 610	1.04	$\overline{\nu_\mu}$	541 592	0.78
e^-	5610	0.0094	e^+	6537	0.011
ν_e	1324	0.0021	$\overline{\nu_e}$	397	0.00091
γ	886 668	1.53	K_L	10 053	0.022

In the used setting of Pythia6, all hadrons apart from protons, neutrons (which are practically stable at the given scales) and, K_L are forced to decay at the same position as the inelastic interaction, without propagating further. Almost all decays into final particles in the sample are two particle decays. As the K_L is stable, interactions with an odd number of K_L have odd multiplicity. Another way to achieve odd multiplicity are photons, which can be produced in quark interactions or emerge in decays such as $\pi^0 \to \gamma e^+ e^-$. Since such processes are rare, it is not surprising that even multiplicities are observed more frequently.

Most of the direct products of the inelastic muon–proton interactions immediately decay into pions, which further decay into either photons or muon–neutrino pairs. Some interactions result in a neutron instead of a proton, or proton and neutron pairs are created, always with baryon number conservation. Thus, $N_{\text{events}} = N_p + N_n - N_{\overline{p}} - N_{\overline{n}}$ where N denotes the quantity of the respective particle.

Electrons are created in pairs, e.g. from $\pi^0 \to e^+e^-\gamma$, or with the corresponding neutrino such as in $K^+ \to e^+\nu_e$, conserving the lepton family number. Also, muon number and charge conservation is always met.

The multiplicity depends on the muon weight: Events with higher multiplicities have been assigned a higher muon weight, with and both variables being linked to the momentum of the incoming muon. High–momentum muons produce more particles, as creation of new particles requires energy. This relation can be seen in Figure 5.2. The momentum is also correlated with the muon weight, because DIS is more likely to occur at higher energies which can break up the proton structure.

Momentum Distribution

The momentum spectrum of the initial muons, the muons after the DIS process and of the other interaction products can be seen in Figure 5.3. In the interactions, the muons keep most of their momentum, and the leftover energy is distributed approximately according to a power law over the created particles.

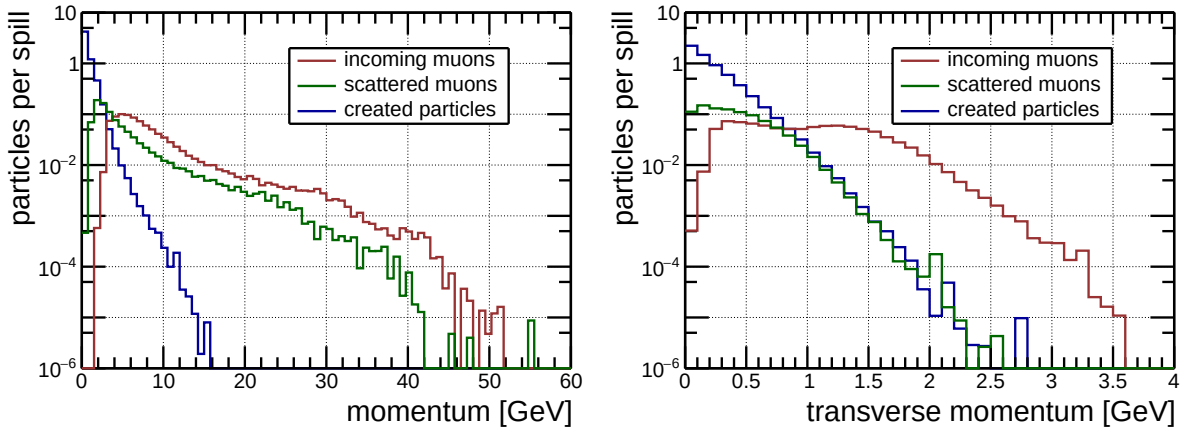

Figure 5.3: Momentum distribution of the Pythia6 sample. The total momentum (left) and the transverse momentum (right) of the incoming muons (red), the outgoing muons after the deep inelastic scattering (green) and the interaction products (blue). After the interaction, most of the momentum is still carried by the muon and the momenta of the products are stochastically distributed. The smaller transverse momentum is almost completely given in the stochastic process, which results in similar curves for the products. Additionally, the effect of the 3 GeV cut to incoming muons is visible.

In general, the x and y components of the momentum are insignificant with respect to the total momentum, but have to be large enough for the muons to hit the off–axis detector. Despite this, low transverse momenta relative to the beam line are observed. This is caused by the muon sweeping system which deflects some of the muons so that the transverse component of the momentum can be close to zero. Another possibility is refraction of the muon in elastic interactions before the DIS, e.g. with the magnets or the vessel, respectively.

Due to its small contribution to the total momentum, most of the transverse component of the incoming muon is channeled into the stochastic distribution, resulting in a power law distribution. As a consequence, the transverse momenta of the scattered muons and the other products are very similar, but differ in the small momentum range.

Interaction Position

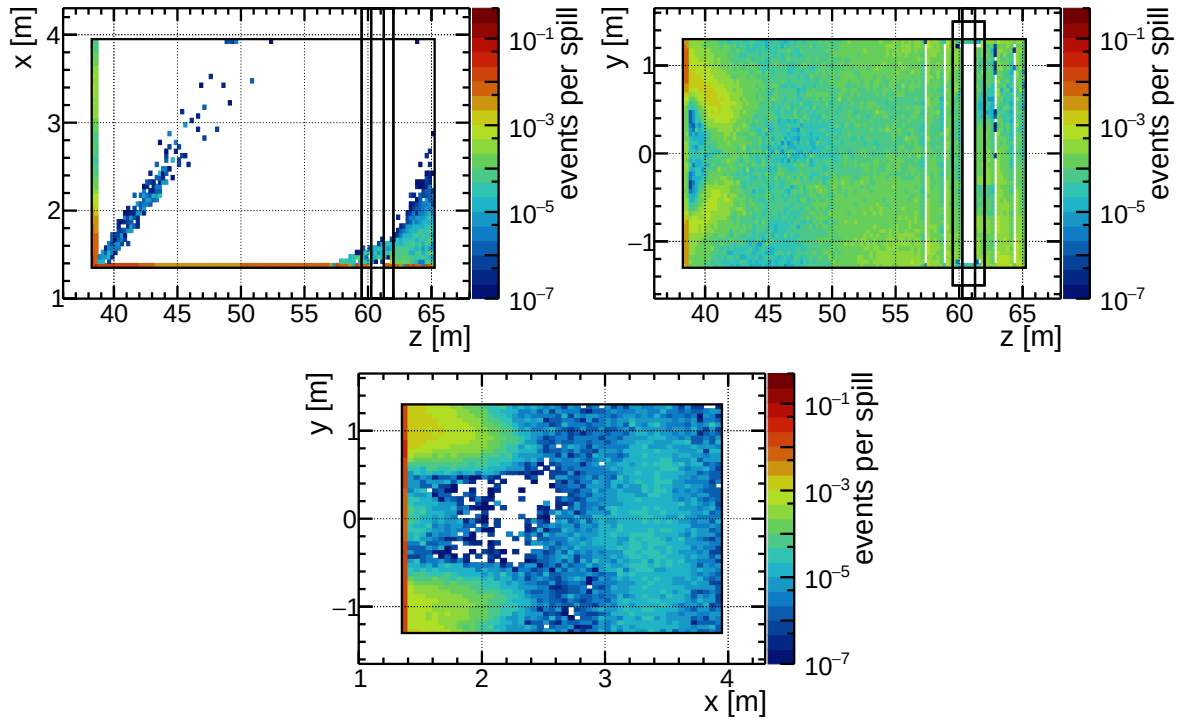

Figure 5.4: Interaction position of the muons in the Pythia6 sample. The three dimensional interaction position is projected on the xz–plane (top left), the yz–plane (top right) and the xy–plane (bottom). Since all interactions occur in the 14 mm thick vessel wall, they can also be interpreted as cuts through the plane of one vessel wall: The bottom plot shows the front wall of the vessel, the right plot the side wall next to the beam and the left plot the top and the bottom wall with doubled intensity. The other two walls contain only a handful of events. Clearly visible are the outlines of the dipole magnet and the four tracking stations.

Each inelastic muon scattering event proceeds completely at the location of the DIS. The interaction positions are shown in Figure 5.4, with all interactions occurring in the 14 mm thick decay vessel. Muons and antimuons are split up in y–direction, the upper maxima stem from the antimuons and the lower maxima from the muons.

The shape across the vessel wall shown in the top left plot originates in the upper and lower vessel wall, one solely caused by muons, the other due to only antimuons. These muons have to pass through another vessel wall beforehand due to the geometry of the beam line, but are forced to interact when first entering the vessel. The observed shape is caused by muons, which had undergone inelastic scattering before they interacted again in another vessel wall. Naturally, this occurs mostly in the regions of highest intensity, which explains the observed structure.

The distribution depends weakly on the muon weight, as the shape described above and the corner structure in the top left plot stem from low weight muons. No dependence on muon momentum, transverse momentum, event weight or multiplicity was observed.

Normalization

In order to relate the results of the MC simulation to the real experiment, the number of events is normalised to one spill of $2.0 \cdot 10^{13}$ pot events. Additionally, the number of events in the $2.4 \cdot 10^6$ spills over the SHADOWS lifetime can be calculated according to

$$N_{\text{events}}/\text{spill} = \frac{\sum \text{weights}}{\#\text{simulated pot events}} \frac{\text{pot}}{\text{spill}} \tag{5.1}$$

$$N_{\text{events}}/\text{lifetime} = N_{\text{events}}/\text{spill} \cdot \frac{\text{spills}}{\text{lifetime}} \tag{5.2}$$

with the number of $1.28 \cdot 10^8$ simulated pot events. After summing the corresponding weights, the number of deep inelastic muon interactions $N_{int.}$ per spill and over the entire SHADOWS lifetime is

$$N_{\text{int.}}/\text{spill} = \frac{6.06 \cdot 10^{-6}}{1.28 \cdot 10^8} \cdot 2 \cdot 10^{13} \approx 0.93 \tag{5.3}$$

$$N_{\text{int.}}/\text{lifetime} = 0.93 \cdot 2.4 \cdot 10^6 \approx 2.23 \cdot 10^6 \tag{5.4}$$

5.4 Selection Criteria for Background Reduction

To reduce the background, multiple requirements can be demanded from the data to identify fake FIP vertices. These selection criteria are also employed in the sample to quantify the expected number of remaining events in the experiment.

The different requirements are correlated with each other, e.g. the scattered muon is part of almost all pairs of charged particles above 3 GeV. As a consequence, the selection criteria cannot be applied independently, resulting in a small number of events fulfilling all the demands. The impact of the subsequent selection criteria is summarised in Table 5.4, on the basis of the normalization described above.

Veto system The majority of the interacting muons are registered by the upstream and the lateral veto, which have a detection efficiency of approximately 99.8%. FIPs unlike muons would not generate a signal in the sub–detector, so all events with corresponding hits in the veto system can be excluded. Given that only an insignificant number of muon tracks do not pass through the vetoes, it can be assumed that the veto system reduces the total number of background events by a factor of $2 \cdot 10^{-3}$.

Kinematic selection FIPs are expected to decay differently according to their spin and mass, but the main decay modes are into two photons or a pair of charged leptons, pions or kaons. Thus, to count as a signal, the tracker demands two oppositely charged particle tracks with energies above 3 GeV in the acceptance region. The photons would only be registered in the ECAL, and only affect the ECAL background, which will not be discussed in this thesis. A plot of all tracks at the position of the dipole magnet is depicted in Figure 5.5.

The determination of whether a particle is within the tracker acceptance region is accomplished by demanding the particles to be in the decay volume in the plane of the dipole magnet. This method neglects the effect of the magnet on the tracks and the efficiency of the trackers. Together, these three criteria reduce the number of events significantly by a factor of about 1250. At this point, the majority of pairs consist of two muons, one being the scattered muon, and only a small number of protons or antiprotons.

Vertex requirements and impact parameter When two oppositely charged tracks are detected and meet the timing requirements, the distance of closest approach is used to determine whether they stem from the same vertex. Furthermore, this vertex is required to be located in the decay volume with a gap of at least 2.5 cm from the vessel. This cannot be explored using this MC simulation, because all interaction vertices are located in the vessel, and the reconstruction of tracker hits is not provided by the simulation.

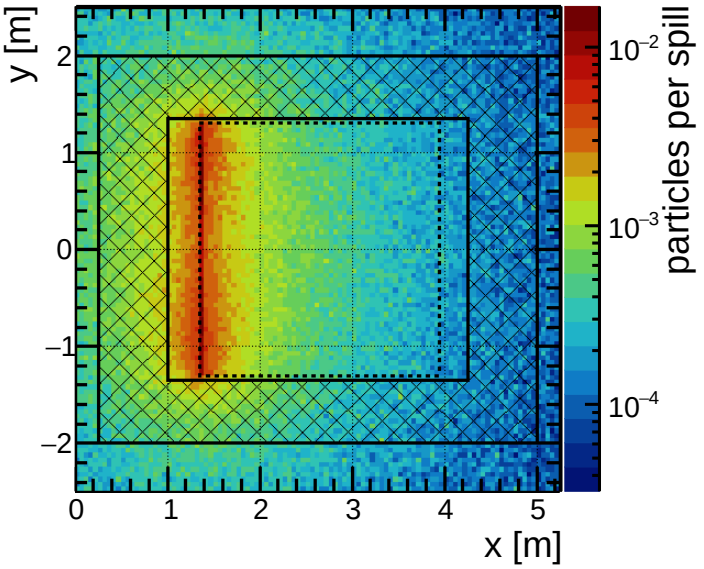

Figure 5.5: Position of the tracks from the Pythia6 sample at the plane of the dipole magnet. The dipole magnet at $z = 60.75\,\mathrm{m}$ is represented by the shaded area, the decay vessel by the dashed line. Most of the tracks originate from the vessel wall next to the beam at $x = 1.35\,\mathrm{m}$ and have a small transverse momentum component.

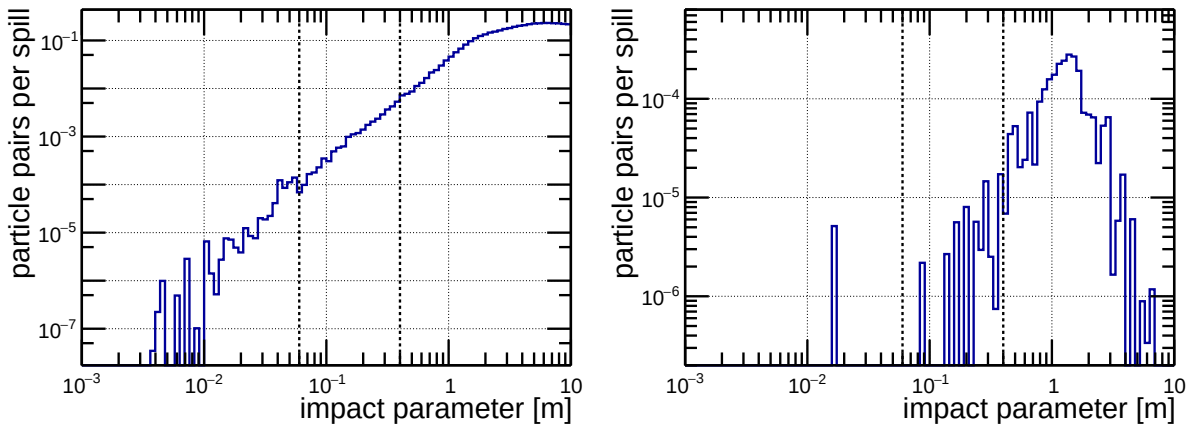

Figure 5.6: Impact parameter of particle pairs of the Pythia6 sample. In both plots, the IP for all particle pairs emerging from the interaction (left) and pairs of oppositely charged particles with momenta above 3 GeV in the tracker acceptance, the required IP for partially and fully recovered tracks is drawn.

The Impact Parameter (IP) of a reconstructed particle track is its smallest distance to the point of interaction. A FIP would originate from the impinging point of the proton beam on the dump. However, the IP of the reconstructed FIPs is expected to be greater than zero, because varying production positions in the dump and the limited precision of the tracking system distort the result. As the FIP decays into multiple particles which may further decay, their momenta add up to the FIP momentum. Therefore, the IP of the reconstructed FIP candidate to the beam dump can be examined, with the requirement of an IP < 6 cm for fully recovered tracks. If only a fraction of the decay products could be reconstructed (e.g. were registered by the tracker), the contribution of the missing particle is assumed to be small and an IP $< 40\,\text{cm}$ is demanded[3]. The IP is shown in Figure 5.6 for all pairs of particles and only for those satisfying the kinematic selection criteria. The remaining events are all muon–antimuon pairs.

Table 5.4: Number of muon background events after applying different selection criteria to the Pythia6 sample. The FIP decays into photons are not considered, and no vertex requirements could be demanded.

$N_{\text{int.}}$	$N_{\text{int.}}$/spill	Requirement (stacked)
711 894	$9.33 \cdot 10^{-1}$	None
711 894	$1.87 \cdot 10^{-3}$	Not vetoed
17 280	$1.55 \cdot 10^{-4}$	Two particles with $p > 3\,\text{GeV}$
1449	$1.41 \cdot 10^{-5}$	Hit the tracker magnet
574	$4.67 \cdot 10^{-6}$	Oppositely charged
21	$1.33 \cdot 10^{-7}$	IP $< 40\,\text{cm}$ (partially recovered tracks)
1	$1.02 \cdot 10^{-8}$	IP $< 6\,\text{cm}$ (fully recovered tracks)

As can be seen in Table 5.4, $1.02 \cdot 10^{-8}$ events per spill are expected for in IP of 6 cm, which is applied for fully reconstructed events. For partially reconstructed events, $1.33 \cdot 10^{-7}$ events per spill are expected where an IP of only 40 cm is demanded. For the whole SHADOWS lifetime, that sums up to $2.45 \cdot 10^{-2}$ and $3.20 \cdot 10^{-1}$ events, respectively.

[3]These numbers are derived from a signal Monte Carlo study, which simulated FIPs of different masses. About 97% of the FIPs have an IP $< 6\,\text{cm}$, while excluding most background events.

5.5 Conclusion

The advantage of the PYTHIA6 sample compared to the GEANT4 sample lies in its large size, which is only possible due to the forced interactions with the vessel. This allows for several selection criteria, which would have been impossible with just a few events. However, the forced interactions also have a drawback, free decays are disregarded completely, and the thickness of the vessel itself is neglected.

Another issue with the sample is that the entire interaction is constrained to be in one location, and that long–living hadrons also decay there, although they may contribute to the background. Additionally, K_{L} could decay into particle pairs of opposite charge, which could contribute to the total number of background events.

However, the simulation aimed to give a rough estimate of the number of background events, achieved through the results presented in Table 5.5.

Table 5.5: Results for the inelastic muon background with the Pythia6 sample. This includes the number of interaction with fully and partially reconstructed events per spill and over the whole SHADOWS lifetime.

$N_{\text{int., fully reconstructed}}$/spill	$1.02 \cdot 10^{-8}$
$N_{\text{int., partially reconstructed}}$/spill	$1.33 \cdot 10^{-7}$
$N_{\text{int., fully reconstructed}}$	$2.45 \cdot 10^{-2}$
$N_{\text{int., partially reconstructed}}$	$3.20 \cdot 10^{-1}$

6 | Analysis of the Geant4 Sample

Another sample has been created with the same output from the BDSIM simulation, using only the GEANT4 software package. Here, muons are not forced to interact, so the number of interactions with the vessel is much lower. Overall, a total of $5.86 \cdot 10^8$ pot events were simulated with the objective of comparing both samples.

6.1 Sample Composition

Similar to the PYTHIA6 sample, the events are saved in a ROOT TTree structure, which allows for simple data storing and manipulation. An event from the GEANT4 sample contains a muon from the TAX dump and its interaction products. For each event, the multiplicity and event weight is stored, along with the particle type, production position and momentum of each particle, similar to the other sample and explained in Table 5.1. Additionally, hits in the different detectors are recorded, but are not used in this study.

One significant difference to the PYTHIA6 sample is that particles are not forced to decay immediately, meaning they propagate some distance and have different production positions.

Table 6.1: A typical event from the Geant4 sample. The antimuon enters the simulation at $z = 38.05\,\text{m}$ and then interacts with a vessel proton in a deep inelastic interaction. A neutral particle like a K_S or ρ–meson is created, which immediately decays into two oppositely charged pions, which then further decay into muon–neutrino pairs after a few meters. There is a potential bug in the simulation, muon antineutrinos are almost exclusively created in free muon decays, but as neutrinos do not play a role in the simulation, this does not pose a problem.

multiplicity		5					
event weight		0.000140144					
part.	x [mm]	y [mm]	z [mm]	p_x [MeV]	p_y [MeV]	p_z [MeV]	E [MeV]
μ^+	1017.65	346.754	38 050	641.966	678.134	6906.22	6969.86
μ^+	1363.61	522.684	41 107.3	0	0	0	105.658
ν_μ	1363.61	522.684	41 107.3	-19.6934	-14.6129	-16.9171	29.7919
μ^-	-8026.67	9166.52	72 320.7	-217.436	184.45	652.727	720.081
ν_μ	-8026.67	9166.52	72 320.7	-97.7268	105.933	394.98	420.454
sum				-976.823	-402.364	-5875.43	-5693.88

An example event from the GEANT4 sample is shown in Table 6.1. In opposition to the PYTHIA6 sample, particles have different production positions. The sample lacks information about the the scattered muon, although its momentum can be calculated over the missing momentum.

The GEANT4 sample is split into 1171 files, each containing the products from 500 000 pot events, giving a total of $5.86 \cdot 10^8$ pot events. Due to the muon biasing, the sample is equivalent to about $9.28 \cdot 10^{11}$ pot events. Approximately $4.63 \cdot 10^8$ muons were produced, of which 41% are muons, 59% antimuons. Other particles like pions and photons enter the simulation in events alongside the muons, they are created after the beam dump e.g. via inelastic interactions with the MIBs. Only $8.09 \cdot 10^5$ of the muons interacted further. The aim is now to identify deep inelastic muon scattering events so that a comparison is possible.

6.2 Identification of Inelastic Muon Interactions

To reproduce and control the results of PYTHIA6, free decays and interaction with any material other than the vessel must to be filtered out. This is done in multiple steps, discussed in detail in the following.

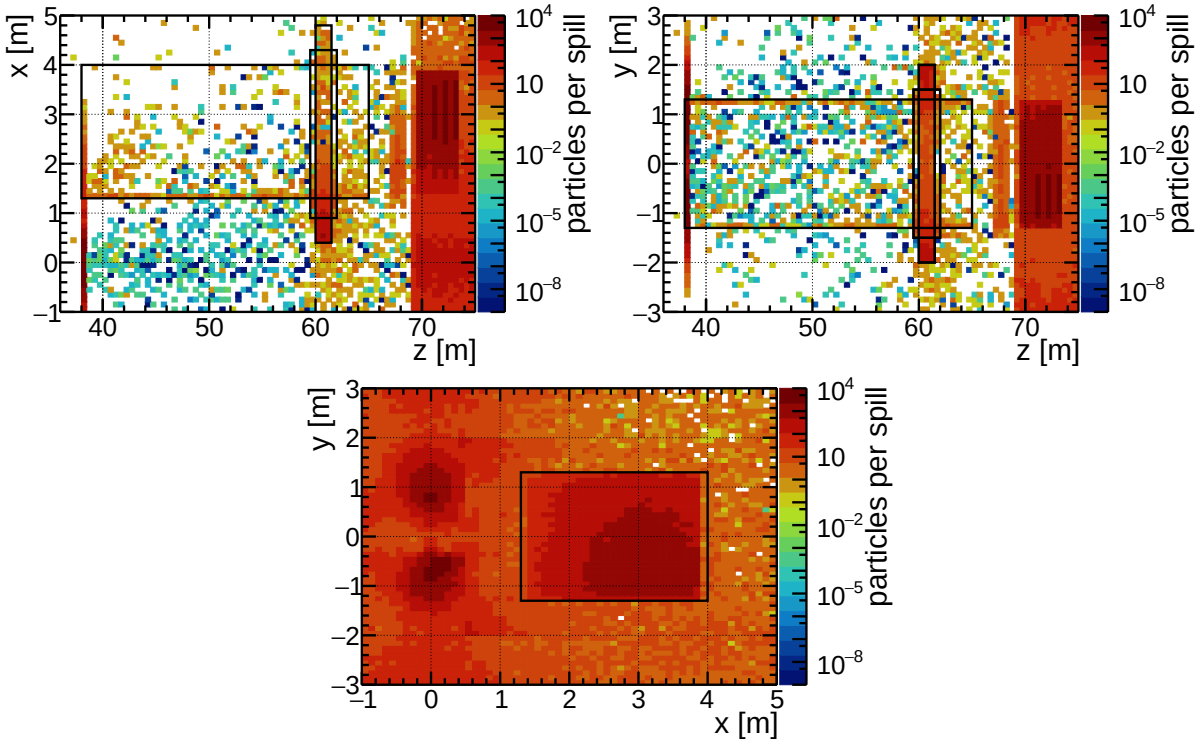

Figure 6.1: Interaction position of the particles in the Geant4 sample. The three dimensional production position is projected on the xz–plane (top left), the yz–plane (top right) and the xy–plane with the dipole magnet outlined. The inelastic vessel interactions are superimposed by several other interactions: Forced free muon decays from 69 m on, interactions with the detectors or other material, and the decay of short–lived particles from the dump.

In Figure 6.1, the production positions of all particles are shown. At $z = 38.05$ m, the initial particles from the beam dump enter the simulation 50 cm before the vessel. The spatial splitting of the muon charges is also noticeable, with the muon trajectories bent in

negative and the antimuon trajectories in positive y–direction. The dipole magnet, the ECAL and the muon system are visible, because many muons interact with the high–Z materials. These scatterings can be identified by their position.

A challenge with the GEANT4 analysis is posed by particles without momentum. They appear in normal interactions, e.g. one or more of the products from $\mu^+ \to e^+\nu_e\overline{\nu_\mu}$. It is assumed that these are internal GEANT4 states that should be ignored or particles which were absorbed later on. As they lack directional information and do not satisfy energy conservation, they are excluded from the following analysis.

Muons are forced to decay through the main decay channel $\mu^+ \to e^+\nu_e\overline{\nu_\mu}$ and $\mu^- \to e^-\overline{\nu_e}\nu_\mu$ from $z = 69\,\mathrm{m}$ to $300\,\mathrm{m}$, occasionally emitting an extra photon. These events can be filtered out by checking the energy conservation in the interaction, i.e. if the momentum of the initial particles does not equal the total product momenta. However, some products of these interactions have no momentum which breaks the energy conservation, and these decays are identified by their products.

The low–weight interactions in the extension of the beam line around $x = y = 0\,\mathrm{m}$ originate from short–lived particles such as pions and kaons. These particles enter the simulation alongside the muons and decay shortly after. In events with multiple initial particles, the weights from all biased particles are multiplied, and thus the weight of the short–lived particles is small. These events are filtered out by demanding a muon to interact.

Following these conditions, the resulting events must be reduced to those that actually occur in the vessel. Unfortunately, the data does not contain the interaction position but only the production position of the final particles. These positions coincide, if the intermediate particles have small lifetimes and propagate a negligible distance, which can be assumed for all decaying particles except for kaons and charged pions (see Figure 2.2). The interaction position can be calculated by extrapolating the tracks of these particles, which are identified by their decay products.

About 74% of the interaction are at z–positions over 75 m, 8% are free muon decays before 75 m, and 0.4% of the events do not exhibit a muon decay at all. Demanding interactions in the vessel which do not contain particles without momentum leaves 119 events, which are depicted in Figure 6.2. Overall, roughly a fifth of the events contain at least one momentumless particle.

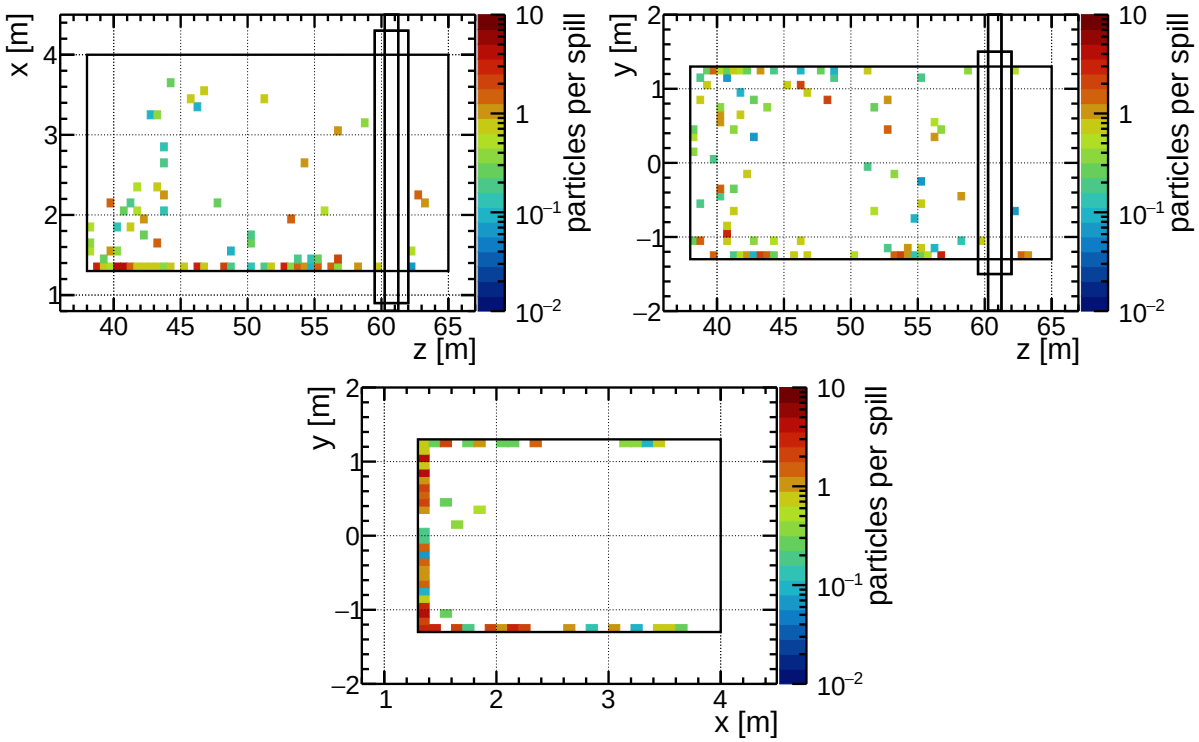

Figure 6.2: Inelastic muon interaction positions in the vessel of the Geant4 sample. The three dimensional production position is projected on the xz–plane (top left), the yz–plane (top right) and the xy–plane with the dipole magnet outlined. After the selection, the events share the same initial conditions as the PYTHIA6 sample, i.e. they are deep inelastic muon interactions with protons from the vessel.

6.3 Comparison with the Pythia6 Sample

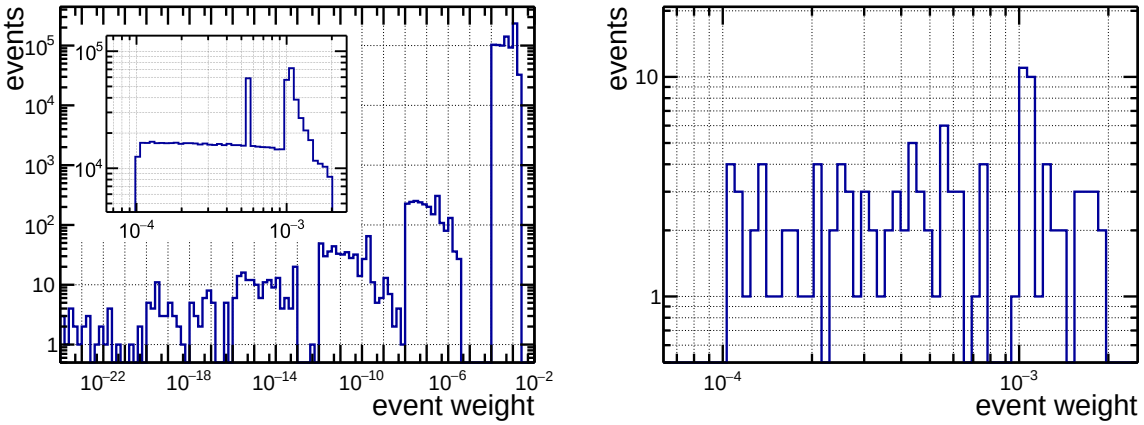

Figure 6.3: Event weights from the Geant4 sample. The distribution of all weights (left) is similar to the one from the PYTHIA6 sample and has a mean of $6.71 \cdot 10^{-4}$. The weights for inelastic muon interactions with the vessel (right) have an average of $6.78 \cdot 10^{-4}$.

With the selected events, it is now possible to compare the two samples. Overall, a number of 1.75 inelastic muon interactions per spill was calculated, which is in the same order of magnitude as the 0.93 events per spill from the PYTHIA6 sample. Over the whole SHADOWS lifetime, this sums up to $4.19 \cdot 10^6$ events.

Event weight

The event weight, depicted in Figure 5.1 and Figure 6.3, exhibit the same features in both samples, multiple blocks for different numbers of initial particles. Each block has the same structure with a decrease for smaller weights and a distinct peak best seen in the first block. This structure originates from the weight window algorithm described in [30]. The GEANT4 sample contains more events in the range of the first block, and thus the average weight is slightly higher for interacting particles, $6.78 \cdot 10^{-4}$ compared to the $6.29 \cdot 10^{-4}$ from the PYTHIA6 sample. Due to the small sample size is it difficult to compare these numbers with the vessel interactions from the GEANT4 sample, but at least the averages show accordance.

Multiplicity, vertices and particle content

Regarding the particle multiplicities, the two samples diverge, as can be seen in Figure 5.2 and Figure 6.4. In the PYTHIA6 sample, 6.5 particles are created on average not counting the resting proton, whilst the mean in the GEANT4 distribution is 3.4 particles. However, the maximum of 3 outgoing particles and the more probable creation of an even number of products are reflected by both samples.

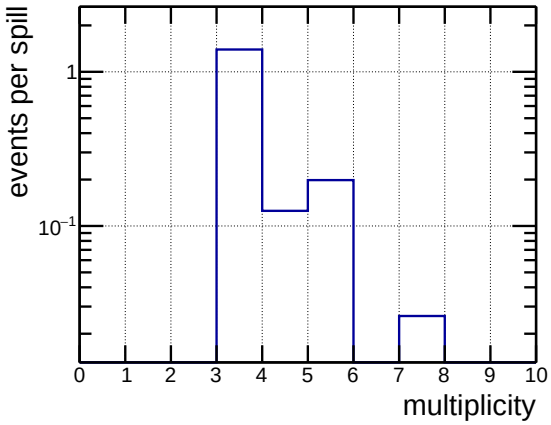

Figure 6.4: Multiplicity of the Geant4 sample. The average of the distribution is 3.4 particles, counting the initial muon but not the proton.

Most of the interaction products in both samples are multiple photons pairs or muon–neutrino pairs, which occur with approximately equal probability. In the GEANT4 sample, 78% of the events produce exactly one of these pairs, 16% two pairs and 0.8% three pairs. All other events include electrons. As expected from the higher mean multiplicity, more pairs are created on average in the PYTHIA6 sample. There, 11% of the interactions produce one of the pairs, 53% two pairs, 20% three pairs and 16% more pairs, but single emitted photons from the quark process and K_{L} distort these numbers slightly.

Comparing the particle contents shown in Table 5.3 and Table 6.2, more photons were created in PYTHIA6, and the GEANT4 sample lacks muon antineutrinos. Additionally, a significantly higher number of electrons are produced in the GEANT4 sample relative to the incoming muons, and no kaons or pions were produced. Both samples emphasise that most of the particles created in the inelastic muon interactions are photons, muons and muon neutrinos.

Table 6.2: Particle content of the Geant4 sample. The muons that interacted are also included, unlike the protons.

particle	number	number/spill
γ	81	1.20
μ^-	119	1.70
μ^+	98	1.38
ν_μ	98	1.33
$\overline{\nu_\mu}$	0	0
e^-	5	0.13
e^+	5	0.13

Interaction position

The positions of the muon–proton interactions are depicted in Figure 5.4 and Figure 6.2. Both show similar distributions, most of the interactions take place in the side wall of the vessel facing the beam line. The structures seen in the xz– and yz–planes of the PYTHIA6 sample can be identified in the other sample as well, but are more spread out.

The PYTHIA6 sample contains much more scatterings with the front wall of the decay vessel, about 28.1%, in comparison to 3.4% in the GEANT4 sample. Possible reasons for this might be the mechanism of the forced muon interactions or the algorithm that extrapolates the tracks from the charged pions back to the interaction position.

Momentum distribution

The number of inelastic vessel interactions in the GEANT4 sample is too small for a comparison with the momentum distribution of the PYTHIA6 sample. The average momentum of the incoming muons is 4.85 GeV in the GEANT4 sample and significantly higher in the PYTHIA6 sample with 8.93 GeV. The scattered muon has with 20.4% and 40.2% lost a very different amount of energy, which may be connected to the energy of the incoming muon. Additionally, the mean energy of the created particles shows with 0.17 GeV and 0.61 GeV a large discrepancy. None of the created particles have momenta greater than 2 GeV in the GEANT4 sample.

Similarly, the transverse momentum of the incoming muons is 0.75 GeV and 0.77 GeV on average for the GEANT4 and PYTHIA6 sample, 0.47 GeV and 0.34 GeV for the scattered muons, and 0.19 GeV and 0.21 GeV for the newly created particles.

Opening angle

In this context, the opening angle is the angle of the smallest cone containing all particles leaving the interaction, which is also the largest angle between two tracks. In the GEANT4 sample, the average opening angle is 43.5° in contrast to 75.3° in the PYTHIA6 sample. A reason might be the higher multiplicity of the particles in the PYTHIA6 sample, as well as the different production positions in the GEANT4 sample. Only considering the particles with momenta greater than 3 GeV, the average opening angle is only 0.16°.

6.4 Conclusion

The aim of the analysis of the GEANT4 sample was to have an independent simulation in order to validate the results obtained from PYTHIA6. It was limited by the small amount of inelastic muon scatterings with the vessel in the GEANT4 sample, which did not force interactions with the vessel unlike the other simulation. However, the results of 1.75 events per spill and $4.19 \cdot 10^6$ events over the whole SHADOWS lifetime are in accordance with the 0.93 events per spill and $2.23 \cdot 10^6$ events over the SHADOWS lifetime from the PYTHIA6 sample.

The lower momenta of incoming muons entailed a lower multiplicity, a different momentum spectrum of the products, a different distribution of particle occurrences and the opening angle of the products. The interaction position of the muons in both samples was similar.

It should be noted, that a deeper analysis of both samples will be done in the Technical Design Report, which will be prepared if SHADOWS is approved. The comparison of the samples, the method of forcing muons to interact and the impact of pions and kaons will be investigated in detail.

7 | Summary

Recently, the SHADOWS experiment was proposed as a beam dump experiment aiming to probe for FIPs in the range of MeV to GeV with an off–axis detector. In the course of the Technical Proposal, the background component arising from inelastic muon interactions with the surrounding material was investigated. Therefore, a Monte Carlo simulation sample with the Pythia6 generator was created, in which interactions with the decay vessel were induced artificially. Most of the relevant scatterings are supposed to happen there, and forcing the interaction significantly increases the size of the data set. Another sample created with the Geant4 software package without the forced interaction as comparison for the results of the other simulation. As one of the key features of Pythia6 are high–energy interactions with protons involving strange and charm quarks, Geant4 is more specialised on the passage of lighter particles through matter.

The analysis of the Pythia6 sample yields $2.23 \cdot 10^6$ deep inelastic muon interactions with protons of the decay vessel, which can result in new particles mimicking the signal from FIP decays. It relies on the final particle algorithm for distinguishing between final decay products and intermediate particles. Similar to the filtering of real data in the experiment, multiple requirements can be demanded from the simulated events: Two oppositely charged particles with a minimal momentum of 3 GeV have to hit the trackers with a small impact parameter. Additionally, a veto system detects incoming muons, so that the number of background events is reduced by 8 orders of magnitude to $2.45 \cdot 10^{-2}$ events for fully reconstructed and $3.20 \cdot 10^{-1}$ events for partially reconstructed vertices. The numbers and plots in this chapter were published in the Technical Proposal.

Comparing these numbers but also the nature of the interactions with the Geant4 sample showed acceptable agreement. Although inelastic muon interactions are not forced, the $4.19 \cdot 10^6$ events over the SHADOWS lifetime are in accordance with the Pythia6 sample. The energies of the incoming muons were observed to be lower, which resulted in a lower multiplicity, the momentum spectrum of the products to be shifted to lower energies and deviating opening angles. However, the interaction positions of the muons are similar. Due to the small sample size, it was not feasible to apply the same selection criteria as to the Pythia6 sample.

Muons account for the largest background component of the SHADOWS experiment, in the form of inelastic interactions and coinciding detector hits. This results in an expected total background of less than $2.6 \cdot 10^{-2}$ events for fully reconstructed and 1.6 events for partially reconstructed vertices. A discovery of new particles with 90% confidence level would correspond to the observation of 2.3 signal events.

After the Expression of Interest in January 2022 and the Letter of Intent in November 2022, the Technical Proposal handed in by the end of October 2023 will be the last publication before the the SPS committee gives a recommendation about which experiment to chose. The final decision from the CERN Research Board will be made public in December 2023, either the SHADOWS/HIKE setup or the SHiP experiment [34] will be selected.

Bibliography

[1] The SHADOWS Collaboration. *SHADOWS Technical Proposal*. Tech. rep. Geneva: CERN, 2023. URL: https://cds.cern.ch/record/2878470.

[2] Mark Thomson. *Modern Particle Physics*. Cambridge University Press, 2013. ISBN: 9781107034266. DOI: 10.1017/CBO9781139525367.

[3] Particle Data Group. *The Review of Particle Physics (2023)*. URL: https://pdglive.lbl.gov/Viewer.action. (8 Oct. 2023).

[4] Peter W. Higgs. "Broken Symmetries and the Masses of Gauge Bosons". In: *Phys. Rev. Lett.* 13 (16 Oct. 1964), pp. 508–509. DOI: 10.1103/PhysRevLett.13.508. URL: https://link.aps.org/doi/10.1103/PhysRevLett.13.508.

[5] LHCb Collaboration. "Observation of structure in the J/ψ-pair mass spectrum". In: *Science Bulletin* 65.23 (Dec. 2020), pp. 1983–1993. DOI: 10.1016/j.scib.2020.08.032. URL: https://arxiv.org/abs/2006.16957.

[6] LHCb Collaboration. "Observation of $J/\psi p$ resonances consistent with pentaquark states in $\Lambda_b^0 \to J/\psi K^- p$ decays". In: *Physical Review Letters* 115.7 (Aug. 2015). DOI: 10.1103/physrevlett.115.072001. URL: https://arxiv.org/abs/1507.03414v1.

[7] SNO Collaboration. "Direct Evidence for Neutrino Flavor Transformation from Neutral-Current Interactions in the Sudbury Neutrino Observatory". In: *Phys. Rev. Lett.* 89 (1 June 2002), p. 011301. DOI: 10.1103/PhysRevLett.89.011301. URL: https://arxiv.org/abs/nucl-ex/0204008.

[8] BSM Working Group. "Physics beyond colliders at CERN: beyond the Standard Model working group report". In: *Journal of Physics G: Nuclear and Particle Physics* 47.1 (Dec. 2019), p. 010501. DOI: 10.1088/1361-6471/ab4cd2. URL: https://arxiv.org/abs/1901.09966.

[9] Lars Bergström. "Dark matter candidates". In: *New Journal of Physics* 11.10 (Oct. 2009), p. 105006. DOI: 10.1088/1367-2630/11/10/105006. URL: https://arxiv.org/abs/0903.4849.

[10] C. S. Wu et al. "Experimental Test of Parity Conservation in Beta Decay". In: *Phys. Rev.* 105 (4 Feb. 1957), pp. 1413–1415. DOI: 10.1103/PhysRev.105.1413. URL: https://link.aps.org/doi/10.1103/PhysRev.105.1413.

[11] Richard Massey et al. "Dark matter maps reveal cosmic scaffolding". In: *Nature* 445 (Jan. 2007), pp. 286–290. DOI: 10.1038/nature05497. URL: https://arxiv.org/abs/astro-ph/0701594.

[12] Claire Antel et al. "Feebly Interacting Particles: FIPs 2022 workshop report". In: May 2023. eprint: 2305.01715. URL: https://arxiv.org/pdf/2305.01715v1.

[13] Bob Holdom. "Two U(1)'s and ϵ charge shifts". In: *Physics Letters B* 166.2 (1986), pp. 196–198. DOI: https://doi.org/10.1016/0370-2693(86)91377-8. URL: https://www.sciencedirect.com/science/article/pii/0370269386913778.

[14] Marco Ernesto Renato Fabbrichesi, Emidio Gabrielli, and Gaia Lanfranchi. *The Dark Photon*. Springer International Publishing, May 2020. DOI: 10.1007/978-3-030-62519-1. URL: https://arxiv.org/abs/2005.01515.

[15] Joerg Jaeckel, Martin Jankowiak, and Michael Spannowsky. "LHC probes the hidden sector". In: *Physics of the Dark Universe* 2.3 (Sept. 2013), pp. 111–117. DOI: 10.1016/j.dark.2013.06.001. URL: https://arxiv.org/abs/1212.3620.

[16] Gaia Lanfranchi, Maxim Pospelov, and Philip Schuster. "The Search for Feebly Interacting Particles". In: *Annual Review of Nuclear and Particle Science* 71.1 (2021), pp. 279–313. DOI: 10.1146/annurev-nucl-102419-055056. URL: https://arxiv.org/abs/2011.02157.

[17] P. Agrawal et al. "Feebly-interacting particles: FIPs 2020 workshop report". In: vol. 81. 11. Springer Science and Business Media LLC, Nov. 2021. DOI: 10.1140/epjc/s10052-021-09703-7. URL: https://arxiv.org/abs/2102.12143.

[18] The HIKE Collaboration. *High Intensity Kaon Experiments (HIKE) at the CERN SPS: Proposal for Phases 1 and 2*. Tech. rep. Geneva: CERN, Oct. 2023. URL: https://cds.cern.ch/record/2878543.

[19] Debasish Banerjee et al. "The North Experimental Area at the Cern Super Proton Synchrotron". In: (July 2021). URL: https://cds.cern.ch/record/2774716.

[20] Luigi Di Lella and Carlo Rubbia. "The Discovery of the W and Z Particles". In: *60 Years of CERN Experiments and Discoveries*, pp. 137–163. DOI: 10.1142/9789814644150_0006. URL: https://cds.cern.ch/record/2103277/files/9789814644150_0006.pdf.

[21] Fabienne Landua. *The CERN accelerator complex layout in 2022. Complexe des accélérateurs du CERN en janvier 2022*. General Photo. June 2022. URL: https://cds.cern.ch/record/2813716. (25 Sep. 2023).

[22] The SHADOWS Collaboration. *SHADOWS Letter of Intent*. Tech. rep. Geneva: CERN, 2022. URL: https://cds.cern.ch/record/2839484.

[23] The NA62 Collaboration. *NA62: Technical Design Document*. Tech. rep. Geneva: CERN, 2010. URL: https://cds.cern.ch/record/1404985.

[24] Gaia Lanfranchi. *Status and plans of the SHADOWS project*. Sept. 2023. URL: https://indico.cern.ch/event/1303571/contributions/5482376/attachments/2708706/4703125/SHADOWS_SPSC_Sept2023.pdf.

[25] Piet Wertelaers. *SHADOWS Integrated Vacuum Vessel, First design thoughts*. Tech. rep. Geneva: CERN, Apr. 2023. URL: https://indico.cern.ch/event/1246834/contributions/5349414/attachments/2624293/4537905/Vacuum-Tank.pdf. Draft.

[26] Alessandro Balla et al. "Performance of scintillating tiles with direct silicon-photomultiplier (SiPM) readout for application to large area detectors". In: *Journal of Instrumentation* 17.01 (Jan. 2022), P01038. DOI: 10.1088/1748-0221/17/01/p01038. URL: https://arxiv.org/abs/2109.08454.

[27] Stefano Agostinelli et al. *Geant4—a simulation toolkit*. 3. 2003, pp. 250–303. DOI: 10.1016/S0168-9002(03)01368-8. URL: https://www.sciencedirect.com/science/article/pii/S0168900203013688.

[28] John Allison et al. *Recent developments in Geant4*. 2016, pp. 186–225. DOI: 10.1016/j.nima.2016.06.125. URL: https://www.sciencedirect.com/science/article/pii/S0168900216306957.

[29] Laurence Nevay et al. *BDSIM: An accelerator tracking code with particle–matter interactions*. Elsevier BV, July 2020, p. 107200. DOI: 10.1016/j.cpc.2020.107200. URL: https://arxiv.org/abs/1808.10745.

[30] Stefan Ghinescu et al. "A biased MC for muon production for beam-dump experiments". In: *The European Physical Journal C* 81.8 (Aug. 2021). DOI: 10.1140/epjc/s10052-021-09541-7. URL: https://arxiv.org/abs/2106.01932v2.

[31] Torbjörn Sjöstrand, Stephen Mrenna, and Peter Skands. *PYTHIA 6.4 physics and manual*. 05. Springer Science and Business Media LLC, May 2006, pp. 026–026. DOI: 10.1088/1126-6708/2006/05/026. URL: https://arxiv.org/abs/hep-ph/0603175.

[32] Ilka Antcheva et al. "ROOT – A C++ framework for petabyte data storage, statistical analysis and visualization". In: *Computer Physics Communications* 180.12 (Dec. 2009), pp. 2499–2512. DOI: 10.1016/j.cpc.2009.08.005. URL: https://arxiv.org/abs/1508.07749.

[33] Frank Krauss et al. *45. Monte Carlo Particle Numbering Scheme*. Aug. 2021. URL: https://pdg.lbl.gov/2023/mcdata/mc_particle_id_contents.html. (10 Oct. 2023).

[34] The SHiP Collaboration. *BDF/SHiP at the ECN3 high-intensity beam facility*. Tech. rep. Geneva: CERN, Oct. 2023. URL: https://cds.cern.ch/record/2878604.

Acknowledgements

At the very end of this thesis, I would like to thank those persons, without whom this work would not have been possible in this form.

Firstly, I would like to thank my supervisor Rainer Stamen for always taking the time to answer the dozens of questions I buried him under and proofreading this whole work even late at night.

I am really grateful for Prof. Schultz–Coulon for offering me a chance to experience the development of a new experiment, which 'is special even if you spend a life in particle physics', as I was told.

I would also like to thank Prof. Hansmann–Menzemer, who kindly agreed to take the role of the second referee.

Thanks to Tobias, for explaining to me all the strange stuff that particle physicists tend to use, like `ROOT`, the `farm` and the r3 printer.

Also, many thanks to Torben, for companionship in the SHADOWS section and the discussions about what would be reasonable to do next. Thanks again for Rainer for actually clarifying what was reasonable.

I would like to thank Anna for her partial success in keeping my working times reasonable and for shopping an office plant with me.

Then, I am really grateful for Celina, Rainer, Anna, Tobias and my father for reading large parts of this work, keeping an overview of the structure and finding many, many spelling mistakes. In addition, I would like to thank Felix, Varsiha, Mathias, Anke, Lisa and Konrad for reading some parts in detail and discussing the physics behind it.

Finally, many thanks to Gaia and Stefano from the SHADOWS Collaboration, who willingly answered questions, checked numbers and explained to me how simulations are evaluated in detail, even though they had to finish the proposal in parallel.

Erklärung

Ich versichere, dass ich diese Arbeit selbstständig verfasst und keine anderen als die angegebenen Quellen und Hilfsmittel benutzt habe.

Heidelberg, den 03. November 2023